Differences between outward currents of human atrial and subepicardial ventricular myocytes

Gregory J. Amos, Erich Wettwer, Franz Metzger, Qi Li, Herbert M. Himmel and Ursula Ravens*

Institut für Pharmakologie, Universität-GH Essen, Hufelandstrasse 55, 45122 Essen, Germany

1. Outward currents were studied in myocytes isolated from human atrial and subepicardial ventricular myocardium using the whole-cell voltage clamp technique at 22 °C. The Na^+ current was inactivated with prepulses to −40 mV and the Ca^{2+} current was eliminated by both reducing extracellular [Ca^{2+}] to 0·5 mM and addition of 100 μM $CdCl_2$ to the bath solution.

2. In human myocytes, three different outward currents were observed. A slowly inactivating sustained outward current, I_{so}, was found in atrial but not ventricular myocytes. A rapidly inactivating outward current, I_{to}, of similar current density was observed in cells from the two tissues. An additional uncharacterized non-inactivating background current of similar size was observed in atrial and in ventricular myocytes.

3. I_{to} and I_{so} could be differentiated in atrial myocytes by their different kinetics and potential dependence of inactivation, and their different sensitivities to block by 4-aminopyridine, suggesting that two individual channel types were involved.

4. In atrial cells, inactivation of I_{to} was more rapid and steady-state inactivation occurred at more negative membrane potentials than in ventricular cells. Furthermore, the recovery of I_{to} from inactivation was slower and without overshoot in atrial myocytes. In addition, 4-aminopyridine-induced block of I_{to} was more efficient in atrial than in ventricular cells. These observations suggest that the channels responsible for atrial and ventricular I_{to} were not identical.

5. We conclude that the differences in outward currents substantially contribute to the particular shapes of human atrial and ventricular action potentials. The existence of I_{so} in atrial cells only provides a clinically interesting target for anti-arrhythmic drug action, since blockers of I_{so} would selectively prolong the atrial refractory period, leaving ventricular refractoriness unaltered.

The action potential shape shows characteristic differences between atrium and ventricle in several animal models, e.g. the guinea-pig (Hume & Uehara, 1985). Inhomogeneities in repolarizing currents between atria and ventricles generated these action potential shape differences. The action potential of human atrium is markedly shorter than that of ventricle, and possesses no clear plateau phase (Trautwein, Kassebaum, Nelson & Hecht, 1962). A careful comparison between the outward currents of human atrial and ventricular myocytes has, however, not been undertaken.

The transient outward current (I_{to}) is a major repolarizing current in both human atrium (Escande, Coulombe, Faivre, Deroubaix & Coraboeuf, 1987; Shibata, Drury, Refsum, Aldrete & Giles, 1989) and human ventricle (Beuckelmann, Näbauer & Erdmann, 1993; Näbauer, Beuckelmann & Erdmann, 1993; Wettwer, Amos, Gath, Zerkowski, Reidemeister & Ravens, 1993; Wettwer, Amos, Posival & Ravens, 1994). In human atrial myocytes, both Ca^{2+}-dependent and -independent transient outward currents have been described (Escande *et al.* 1987). At room temperature, the Ca^{2+}-independent current did not completely inactivate, even with long depolarizing pulses. This late current could either represent non-inactivating I_{to}, a delayed rectifier, a second distinct current or any combination of these possibilities. Non-inactivating I_{to} should be blocked by 4-aminopyridine (4-AP) at the same

* To whom correspondence should be addressed.

concentrations as the inactivating component of the current. A delayed rectifier has been observed in both atrial and ventricular myocytes, but at physiological and not at room temperature (Beuckelmann *et al.* 1993; Wang, Fermini & Nattel, 1993*a*). This current was not sensitive to 4-AP but could be blocked by tetraethylammonium (TEA; Wang *et al.* 1993*a*). In the presence of TEA, an additional sustained outward current was discovered in human atrial myocytes (Wang, Fermini & Nattel, 1993*b*). However, whether such a current in ventricular myocytes exists has not been investigated.

The aim of our study was to characterize outward currents of atrial and ventricular cells from human hearts, in order to determine the basis for the differences in action potential shapes. Because of the known variations in outward currents of cells from different locations within the ventricular wall (Liu, Gintant & Antzelevitch, 1993), subepicardial myocytes were used in the present study, since these cells exhibit the largest transient outward currents in human myocytes (Wettwer *et al.* 1994). Outward currents were characterized using their kinetics and pharmacology. We found evidence for a sustained current component present in atrial myocytes but not ventricular myocytes, and which was not identical with a classical delayed rectifier. The presence of this current only in atrial myocytes could explain the shorter action potential duration of these cells when compared with ventricular myocytes. Significant differences in the kinetics and pharmacology of the transient outward current between atrial and ventricular myocytes could also be demonstrated.

METHODS

Source of human tissue

Right atrial appendages were obtained from forty-one patients (29 males) undergoing coronary bypass surgery (30), valve replacement (8) or correction of atrial septum defects (3). In addition, one right atrial appendage was obtained from a patient undergoing heart transplant following dilative cardiomyopathy. The average age of the patients was 60 ± 2 years (range 9–74 years). Before surgery, patients typically received a nitrovasodilator (isosorbiddinitrate or glyceroltrinitrate; 24 patients), a Ca^{2+} channel blocker (nisoldipine, nifedipine or diltiazem; 17 patients) and a β-adrenoceptor blocker (metoprolol; 11 patients). Other medicaments commonly given were diuretics (furosemide; 8 patients) and cardiac glycosides (β-acetyldigoxin or digitoxin; 7 patients). Two patients having corrective surgery for atrial septal defects received no drugs prior to surgery. All patients received flunitrazepam prior to anaesthesia. Anaesthesia was induced with etomidate, and sustained with a mixture of enflurane/N_2O. Pancuronium was used for skeletal muscle relaxation, and fentanyl was used as an analgesic.

Left ventricular wall was obtained from explanted hearts of twelve patients (9 males) undergoing heart transplantation. Ten patients were diagnosed as having dilative cardiomyopathy (New York Heart Association classification III–IV), one patient as having restrictive cardiomyopathy and one patient required heart transplantation following complication of an aorto-coronary venous bypass operation. The average age of the patients was 52 ± 5 years (range 17–63 years). Transplant recipients typically received a cardiac glycoside (β-acetyldigoxin or digitoxin; 11 patients), angiotensin converting enzyme blockers (captopril or enalapril; 11 patients) and a diuretic (furosemide; 11 patients). Written informed consent was obtained from all patients prior to the surgery and the investigation complies with principles outlined in the Declaration of Helsinki.

Isolation of atrial and ventricular myocytes

The tissue was transported to the laboratory in Tyrode solution (composed of (mM): 127 NaCl, 5·4 KCl, 1·1 $MgCl_2$, 1·8 $CaCl_2$, 0·4 NaH_2PO_4, 22·0 $NaHCO_3$ and 5·0 glucose; saturated with 95% O_2 and 5% CO_2 to give pH 7·4), or in a cardioplegic solution (Custodial; Köhler Chemie, Alsbach, Germany). All atrial tissue was transported to the laboratory within 10 min of removal. The duration of transport for ventricular tissue depended on the location of the transplant (maximum 120 min). The ventricular tissue was transported on ice, whereas the atrial tissue was not cooled.

The atrial tissue was sliced into chunks of approximately 1 mm^3 in nominally Ca^{2+}-free solution (solution A; composed of (mM): 100·0 NaCl, 10·0 KCl, 1·2 KH_2PO_4, 5·0 $MgSO_4$, 50·0 taurine, 20·0 glucose and 5·0 Mops; pH 7·0 adjusted with NaOH). The tissue chunks were stirred at 35 °C for 45 min in collagenase IA (1·0 mg ml^{-1})/protease 24 (0·5 mg ml^{-1}) in solution A, the $[Ca^{2+}]$ being raised stepwise to 0·2 mM. The enzyme solution was then exchanged for collagenase IA (1·0 mg ml^{-1}) in solution A (with $[Ca^{2+}]$ 0·2 mM) and stirring was continued until rod-shaped, striated cells were seen. The duration of the second enzyme exposure (20–60 min) varied depending on cell yield (5–8%). A portion of the enzyme solution was then removed and gently centrifuged (60 *g*) to facilitate cell settling. The supernatant was replaced with solution A, the Ca^{2+} concentration being raised directly to 0·5 mM.

Myocytes from subepicardial ventricular specimens were isolated as previously described (Wettwer *et al.* 1994). As it has been reported that cloned channels have several extracellular sites potentially sensitive to trypsin cleavage (Tamkun, Knoth, Walbridge, Kroemer, Roden & Glover, 1991), protease was substituted for trypsin when isolating ventricular myocytes in a few cell preparations. Since no differences in membrane currents were seen between myocytes isolated with trypsin or protease, the results have been pooled. Only elongated, cross-striated myocytes were used in experiments.

Measurement of membrane currents

Single electrode whole-cell current clamp and voltage clamp techniques were applied using a List EPC-7 amplifier to measure action potentials and membrane currents. pCLAMP software (Axon Instruments) was used for experimental control and analysis. For experiments, cells were placed into a 0·5 ml Plexiglass bath fixed to an inverted microscope. The electrolyte solution in the bath was in contact with the reference electrode via a 150 mM KCl agar bridge to minimize junction potentials. The bath was perfused with a modified Tyrode solution (composed of (mM): 150·0 NaCl, 5·4 KCl, 0·5 $CaCl_2$, 2·0 $MgCl_2$, 10·0 Hepes and 10·0 glucose; pH 7·4 adjusted with NaOH) at 1·5 ml min^{-1}. The electrode solution contained (mM): 130·0 KCl, 4·0 $MgCl_2$, 5·0 $CaCl_2$, 10·0 Hepes, 10·0 EGTA and 4·0 Na_2ATP, giving a free Ca^{2+} concentration of 50 nM and a free Mg^{2+} concentration of

Table 1. Comparison of the passive electrophysiological properties of atrial myocytes, and of subepicardial ventricular myocytes of human hearts

Parameter	Cell capacitance (pF)	Membrane resistance (GΩ)	Measured resting membrane potential § (mV)
Atrium ($n = 145$)	148 ± 5*	$1{\cdot}85 \pm 0{\cdot}39$* ($n = 54$)	-33 ± 1*
Ventricle ($n = 39$)	285 ± 17*	$0{\cdot}10 \pm 0{\cdot}04$* ($n = 20$)	-56 ± 3*

Values presented as means ± S.E.M. from n cells; * $P < 0{\cdot}05$; § values obtained with electrodes of 2–3 MΩ and an average seal resistance of $4{\cdot}3 \pm 0{\cdot}7$ GΩ.

300 μM. Electrodes were fabricated from filamented borosilicate glass (Hilgenberg Co., Malsfeld, Germany). Experiments were performed at 22 °C unless otherwise specified.

For the measurement of action potentials, we have used electrodes with smaller tip diameters (resistance 8–10 MΩ when filled with electrode solution) in order to obtain high resistance cell membrane–electrode seals (~15 GΩ) and therefore more stable resting membrane potentials. Electrodes with larger tip diameters (resistance 2–3 MΩ) were used to measure membrane currents. With these electrodes, the quality of the seal was markedly reduced (~4 GΩ); however, membrane currents of approximately 2 nA could be measured without large voltage drops.

To gain an estimate of cell size, the cell capacitance was measured before compensation using depolarizing ramps (1 V s^{-1}) from −40 to −35 mV. The respective values are given in Table 1. As membrane conductance is very low and constant in this range (Escande *et al.* 1987), any change in current level is due to the capacitive properties of the cell membrane. Up to 100 pF of the cell capacitance and 60% of the access resistance was then compensated. In a representative group of fifty atrial cells, the initial access resistance was $5{\cdot}69 \pm 0{\cdot}54$ MΩ, and this was reduced to $2{\cdot}28 \pm 0{\cdot}22$ MΩ by compensation. Maximum currents measured during a test pulse to +60 mV averaged 2241 ± 139 pA, thus the average error in command potential due to voltage drop across access resistance was $4{\cdot}42 \pm 0{\cdot}35$ mV. The membrane resistance at the resting membrane potential was estimated by measuring the change in current following a 2 s clamp step from −80 to −60 mV with appropriate correction for current flowing through the seal resistance. Clamp protocols are depicted in the figures, and described in the corresponding legends.

To isolate outward currents, Na^+ current (I_{Na}) was inactivated by 25 ms prepulses to −40 mV from the holding potential of −80 mV. Ca^{2+} currents (I_{Ca}) were blocked by $CdCl_2$ (100 μM), a concentration which blocks I_{Ca} by more than 95% in human ventricular myocytes (E. Wettwer, unpublished observations). I_{Ca} was also kept small by using a low extracellular $CaCl_2$ concentration (0·5 mM). Despite these measures we cannot, however, completely rule out contamination by these currents, and therefore statistical comparisons were made at a test potential of +40 mV, where the driving forces for Na^+ and Ca^{2+} ions are small. The use of Cd^{2+} to eliminate I_{Ca} is problematic as extracellular Cd^{2+} alters the kinetics of K^+ currents in animal models (Agus, Dukes & Morad, 1991). Indeed, shifts in the steady-state inactivation curve for human ventricular I_{to} due to Cd^{2+} have already been described (Wettwer *et al.* 1994). The influences of these experimental conditions on current kinetics make extrapolation of the obtained results to the situation *in vivo* difficult. Organic I_{Ca} blockers were not used, as these drugs block K^+ currents (Gotoh, Imaizumi, Watanabe, Shibata, Clark & Giles, 1991) and their block of I_{Ca} is strongly modulated by membrane potential (Sanguinetti & Kass, 1984).

Materials

All enzymes, bovine serum albumin (BSA), TEA, *N*-methyl-D-glucamine and 4-AP were obtained from Sigma. Dendrotoxin (DTX) was obtained from Calbiochem (La Jolla, CA, USA) and charybdotoxin (CTX) was purchased from Research Biochemicals Inc. (Natick, MA, USA). All other chemicals were obtained from commercial suppliers and were of laboratory grade.

Data and statistical analysis

All current amplitudes, except tail currents, were measured as absolute values (means ± S.E.M.). Tail currents were measured at −20 mV, and analysed as the difference between the steady-state current at −20 mV and the tail current amplitude, obtained by extrapolation of a single exponential equation to the start of the clamp step. For analysis of the kinetics of activation, we have subtracted the capacitive transient and background currents from the original current tracings. To do this, a single exponential function was fitted to the capacitive transient and the extrapolated capacitive 'spike' and background current were then digitally subtracted from the current recording. Fitting of equations to experimental data was performed using pCLAMP software or Prism (Graphpad Software, San Diego, CA, USA). Statistical significance was tested using Student's t tests, paired or unpaired as required. Significance was assumed when $P < 0{\cdot}05$.

RESULTS

Passive electrophysiological properties

Significant differences in cell capacitance, membrane resistance and resting membrane potential were observed between isolated atrial and ventricular myocytes (Table 1). Atrial myocytes were smaller in appearance than ventricular myocytes, which was reflected by cell capacitance. Between −80 and −60 mV, the membrane resistance of atrial myocytes was eighteen times larger than that of ventricular myocytes. The measured resting membrane potential of atrial myocytes was significantly more positive than that of ventricular myocytes.

Action potentials

Recording of action potentials proved very difficult in atrial myocytes, despite the use of small tipped electrodes. In only four of forty-three atrial cells (4 hearts) could we obtain a resting membrane potential sufficiently negative to elicit action potentials. At 22 °C, action potentials from

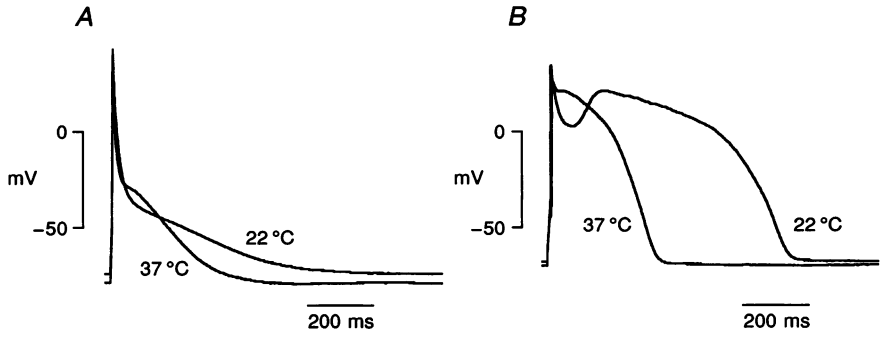

Figure 1. Action potentials from isolated human atrial (*A*) and subepicardial ventricular myocytes (*B*) at 22 and 37 °C

Scaling and zero level indicated; stimulation frequency, 0·2 Hz.

these atrial myocytes were characterized by a very rapid phase 1 repolarization followed by a short plateau phase at −40 mV (Fig. 1*A*). Phase 3 repolarization was slow and the average action potential duration at 90% repolarization (APD_{90}) was 391 ± 32 ms ($n = 4$). Raising the temperature of the bath solution to 37 °C hyperpolarized the resting membrane potential from −61 ± 4 to −64 ± 5 mV ($P = 0{\cdot}046$) and accelerated both phase 1 and phase 3 repolarization, such that the APD_{90} was significantly shortened to 270 ± 42 ms ($P = 0{\cdot}012$). In contrast, action potentials from ventricular myocytes at 22 °C possessed a 'spike and dome' shape, with a marked plateau at positive membrane potentials (Fig. 1*B*). Phase 3 repolarization was slow and the average APD_{90} was 1567 ± 252 ms ($n = 5$). The 'spike and dome' shape disappeared almost completely after raising the temperature to 37 °C in all cells, and in four cells at 37 °C, the average APD_{90} was shortened significantly to 975 ± 325 ms ($P = 0{\cdot}042$). No significant change in resting membrane potential was observed (22 °C, −69 ± 1 mV; 37 °C, −72 ± 2 mV; $n = 5$).

A characterization of the repolarizing membrane currents was undertaken to determine whether inhomogeneity in these currents at least partially underlies the observed differences in action potential shape between atrial and ventricular myocytes.

Quasi-steady-state membrane currents

Quasi-steady-state membrane currents of atrial and ventricular myocytes were measured using a slowly depolarizing ramp from −100 to +40 mV and of 16 s duration. This simple method was chosen because rapidly

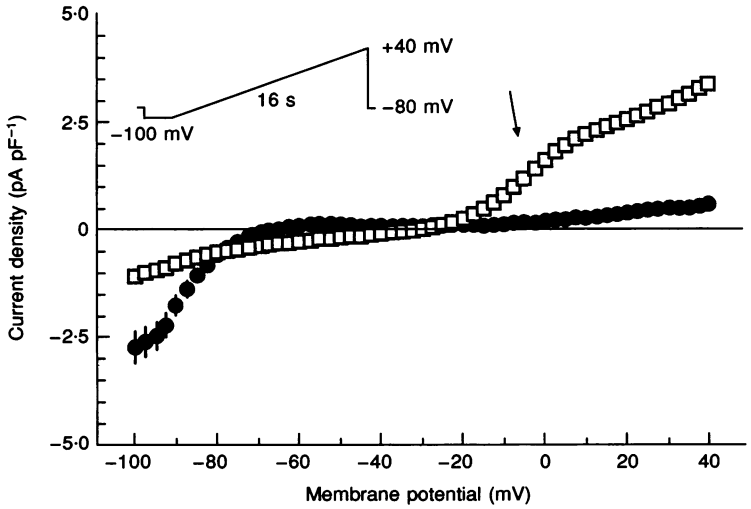

Figure 2. Current–voltage relationships for quasi-steady-state currents of human atrial myocytes (□) and ventricular myocytes (●)

Clamp protocol (inset): slow depolarizing ramp (16 s duration) from −100 to +40 mV. Ordinate: current amplitudes digitized at 2·5 mV intervals and expressed as mean current density ± S.E.M., 50 cells / 9 hearts for atrium, 18 cells / 9 hearts for ventricle. Abscissa: membrane potential during the ramp protocol. The arrow indicates the 'shoulder' in outwardly directed current observed in atrial myocytes only.

activating and inactivating currents should not contribute significantly to the current measured and the ramp pulse is more tolerable for cells than the conventional method of depolarizing test pulses of several seconds duration. To allow for differences in cell size, the digitized current amplitudes were expressed as current densities (pA pF^{-1}) by dividing by the individual cell capacitance. The respective data for atrial and ventricular myocytes are shown in Fig. 2. In atrial cells, the inward current density at −100 mV was 1·1 ± 0·1 pA pF^{-1} (50 cells, 9 hearts). This inward current then declined with depolarization, reversing direction at −36 ± 1 mV. With further depolarization, a 'shoulder' in outward current was observed between approximately −20 and +10 mV (see arrow in Fig. 2). The current density of outward current at +40 mV was 3·4 ± 0·1 pA pF^{-1}. In ventricular myocytes, the inward current density at −100 mV was significantly larger than in atrial myocytes (2·8 ± 0·4 pA pF^{-1}, 18 cells, 9 hearts, $P < 0·01$). With depolarization, the inward current level declined before reversing direction at −57 ± 4 mV. A maximum outward current (0·2 ± 0·03 pA pF^{-1}) was reached at −44 ± 4 mV; the current level then decreased to almost zero with further depolarization. At potentials positive to 0 mV, the outward current level increased slightly and the current density at +40 mV was 0·6 ± 0·1 pA pF^{-1}, which was significantly smaller than the corresponding value in atrial myocytes ($P < 0·01$).

The shoulder in outward current at potentials positive to −20 mV in atrial myocytes only suggests the existence of an extra non- or slowly inactivating outward current at 22 °C in these cells. We have therefore characterized the outward currents in both atrial and ventricular myocytes in further detail.

Activation of outward currents

In human atrial myocytes, various types of outward currents could be differentiated according to their rate and proportion of inactivation (Fig. 3). Most cells possessed a rapidly activating current that inactivated by approximately 50% during the 300 ms test pulse (Fig. 3*B*). A small proportion of cells possessed an outward current that activated quite rapidly but inactivated to only a small degree during the test pulse (Fig. 3*A*). A third group of cells possessed an outward current that activated rapidly and then inactivated almost completely during the test pulse (Fig. 3*C*). The types of outward currents in different cells from the same patient varied, with no connection between medication, diagnosis or patient age being observed. The ratio of the maximum current activated in the test pulse (I_{peak}) and the current remaining at the end of the test pulse (I_{late}) was plotted as a frequency distribution (Fig. 3*D*). The distribution did not exhibit any peaks corresponding to explicit groups. With arbitrary ranges in I_{peak}/I_{late} values, outward current inactivated only slightly ($I_{peak}/I_{late} = 1·0–1·3$) in 22% of cells, incompletely ($I_{peak}/I_{late} = 1·3–2·3$) in 57% of cells, and almost completely ($I_{peak}/I_{late} > 2·3$) in 21% of cells. In ventricular (subepicardial) myocytes, only a prominent inactivating outward current was observed during the

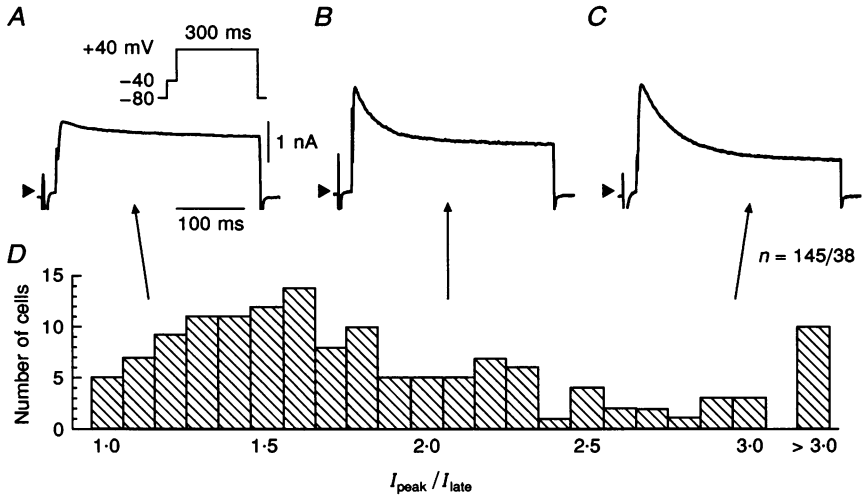

Figure 3. Forms of outward current in human atrial myocytes

A–C, original current recordings of typical outward currents of atrial myocytes activated by a clamp step to +40 mV. Scaling as in *A*; arrowheads indicate zero current level; cell capacitance was 104 pF (*A*), 126 pF (*B*) and 190 pF (*C*). Clamp protocol (inset in *A*): holding potential, −80 mV; 25 ms prepulse to −40 mV; test pulse of 300 ms duration at +40 mV. *D*, frequency distribution for the number of atrial cells encountered (ordinate) with a given quotient (abscissa) of peak outward current amplitude (I_{peak}) to the current remaining at the end of the 300 ms clamp step to +40 mV (I_{late}). Most cells possessed quotients between 1·4 and 2·3 (an example in *B*); however, cells were also encountered with quotients smaller than 1·4 (an example in *A*) and greater than 2·4 (an example in *C*).

test step to +40 mV. The calculated ratio I_{peak}/I_{late} for a test pulse to +40 mV was greater than 2·5 for all cells.

In atrial and ventricular myocytes, outward current was activated by test pulses to potentials positive to −30 mV (Fig. 4). The absolute amplitude of I_{peak} during a test step to +40 mV in atrial myocytes (1552 ± 62 pA, 145 cells, 38 hearts) did not differ from the corresponding value in ventricular cells (1784 ± 174 pA, 39 cells, 11 hearts). However, the amplitude of I_{late} for a 300 ms test pulse was significantly larger in atrial cells (876 ± 37 pA) than in ventricular cells (322 ± 31 pA; $P < 0·01$). When expressed as current densities (pA pF^{-1}), both I_{peak} and I_{late} were significantly larger in atrial than in ventricular myocytes at all test potentials positive to −20 mV (Fig. 4, $P < 0·05$). The current densities at +40 mV of I_{peak} and I_{late} for atrial myocytes were 11·8 ± 0·5 and 6·6 ± 0·3 pA pF^{-1}, respectively. For ventricular myocytes, the corresponding values were 6·1 ± 0·5 and 1·2 ± 0·1 pA pF^{-1}. The current density of the inactivating component (i.e. $I_{peak} - I_{late}$) was, however, not significantly different between the two cell groups (atrium, 5·2 ± 0·4 pA pF^{-1}; ventricle, 4·9 ± 0·4 pA pF^{-1}).

Charge carrier of the outward currents

Substitution of Cs^+ for K^+ in the electrode solution may differentiate between K^+ and Cl^- as charge carrier for outward current, since intracellular Cs^+ should block K^+ but not Cl^- fluxes. In five atrial and ventricular myocytes, only small time-independent outward currents were observed with Cs^+-containing electrode solution. The current density of I_{late} (at +40 mV) was not significantly different between atrial (1·0 ± 0·3 pA pF^{-1}) and ventricular myocytes (1·0 ± 0·4 pA pF^{-1}). The values for atrial cells only were significantly smaller ($P < 0·01$) than those for I_{late} obtained with the K^+-containing electrode solution. These results show that the observed outward currents in both atrial and ventricular myocytes resulted primarily from K^+ fluxes.

Time course of inactivation of outward current

To resolve the time course of inactivation of the total outward current, 2 s test pulses to +40 mV from the holding potential of −80 mV were applied. In fifty-four atrial cells (17 hearts), the time course of inactivation was best described using two exponential functions to account for a rapidly and a slowly declining component. The first

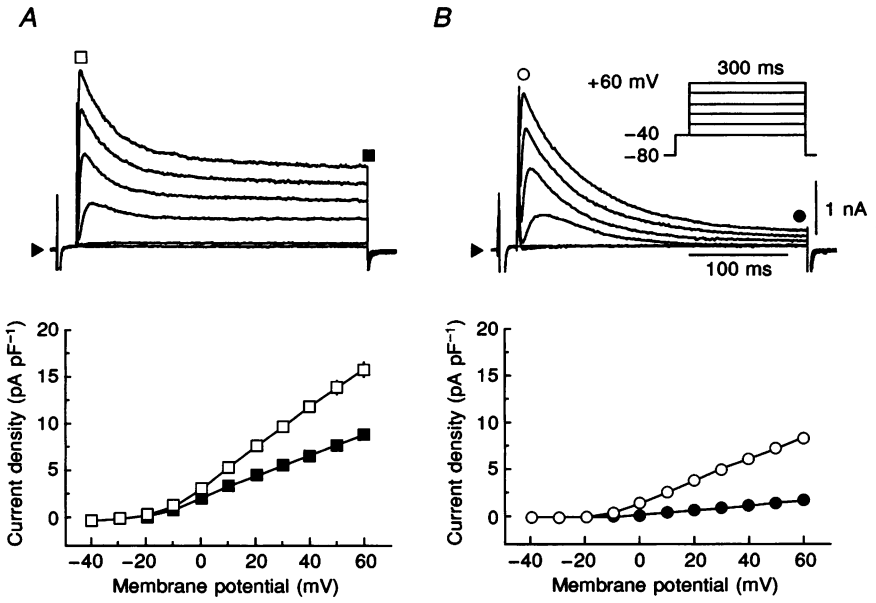

Figure 4. Current–voltage relationships of total outward current of human atrial and ventricular myocytes

A, top: original recording of outward current of the majority of human atrial myocytes. Scaling and clamp protocol as indicated in *B*; arrowhead represents zero current level; cell capacitance was 167 pF. Symbols indicate time of current measurement. Bottom: current–voltage relationship for outward currents of 145 atrial myocytes (38 hearts). Data are expressed as means ± S.E.M. Ordinate: current densities of both peak (I_{peak}, □) and late current (I_{late}, ■). Abscissa: membrane potential of the test pulse. *B*, top: original recording of outward current from a ventricular myocyte. Scaling as indicated; arrowhead represents zero current level; cell capacitance was 302 pF. Clamp protocol (inset): holding potential, −80 mV; 25 ms prepulse to −40 mV; test pulse of 300 ms duration between −40 and +60 mV; increments of 10 mV; frequency, 0·2 Hz. Bottom: current–voltage relationship for outward current of 39 ventricular myocytes (12 hearts). Data expressed as means ± S.E.M. Ordinate: current densities of both peak (I_{peak}, ○) and late current (I_{late}, ●). Abscissa: membrane potential of the test pulse.

component inactivated rapidly with a time constant (τ_{i1}) of 61 ± 1 ms and the second slow component with a time constant (τ_{i2}) of 1425 ± 26 ms. In contrast, in twenty of twenty-one ventricular myocytes (7 hearts), the time course of inactivation was best described using a single exponential function. The average time constant value (τ_{i1}) obtained was 79 ± 2 ms. The τ_{i1} value for the rapidly inactivating component of atrial outward current was significantly smaller than τ_{i1} for ventricular myocytes ($P < 0{\cdot}01$).

Recovery from inactivation of outward currents

Outward currents of both atrial and ventricular myocytes rapidly recovered from inactivation at −100 mV (Fig. 5*A* and *B*). To analyse the time course of recovery from inactivation in both groups, the amplitude of I_{peak} in the

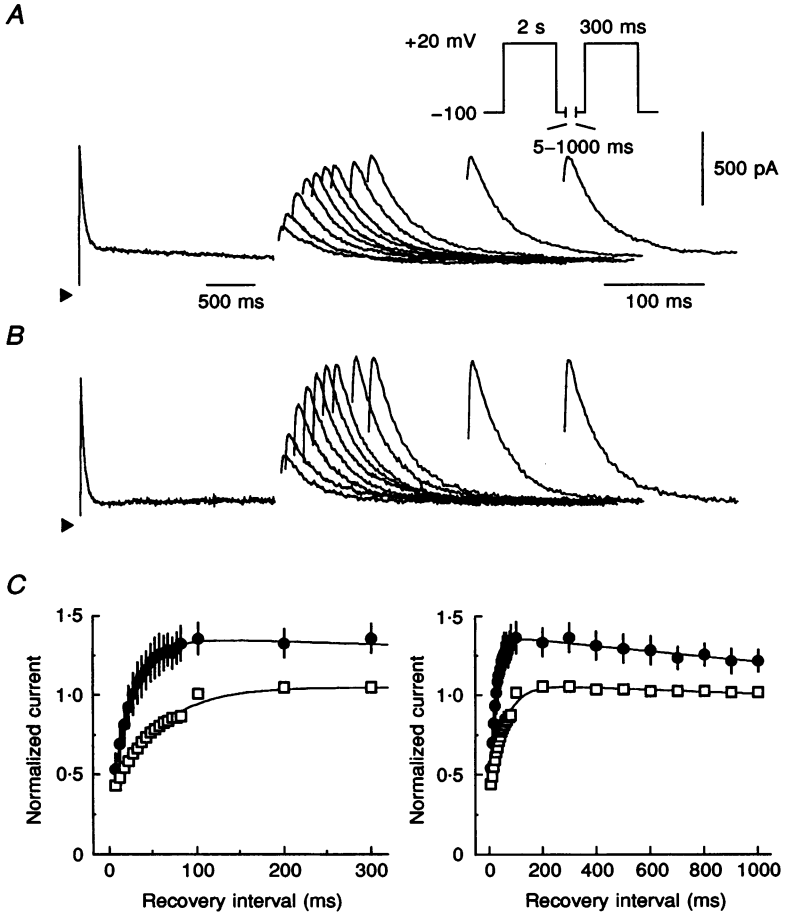

Figure 5. Recovery from inactivation at −100 mV of outward currents of human atrial and ventricular myocytes

A, original recording from an atrial myocyte, current in response to the conditioning pulse is followed by currents elicited by the test pulses. Scaling as indicated (please note the different time scaling between the conditioning pulse and test pulse); arrowhead shows zero current level; cell capacitance was 167 pF. Double pulse protocol (inset): holding potential, −100 mV; 2 s conditioning pulse to +20 mV; recovery intervals between 5 and 1000 ms at −100 mV; 300 ms test pulse to +20 mV; frequency, 0·1 Hz. The tracings show currents measured with recovery intervals between 5 and 300 ms only. *B*, original recording from a ventricular myocyte. Layout as in *A*; cell capacitance was 283 pF. Note the overshoot of the peak current amplitude in the test pulse with respect to the peak current amplitude during the conditioning pulse. *C*, recovery curves for outward current of 6 atrial myocytes (□; 5 hearts) and 7 ventricular myocytes (●; 4 hearts). Ordinate: peak current amplitude in the test pulse normalized to the peak current amplitude in the conditioning pulse (1·0). Abscissa: duration of the recovery interval. Left: data obtained for recovery intervals between 5 and 300 ms; right: data for the full recovery interval range. The equation $I_{test}/I_{cond} = a(1 + \exp(-t/\tau_{ra})) + b(1 - \exp(-t/\tau_{rb}))$ was fitted to the data points, where I_{test}/I_{cond} is the normalized current of the test pulse following a recovery interval of duration t. Component a describes the initial increase in current amplitude with increasing duration of recovery intervals and component b was required to fit the decline in overshoot of ventricular myocytes only.

test pulse was expressed as a fraction of I_{peak} amplitude in the conditioning pulse and plotted against the recovery interval duration. The time course of recovery from inactivation of outward current was slower in atrial than in ventricular myocytes. Peak current of ventricular myocytes showed a clear overshoot of the steady-state amplitude at recovery intervals of about 100 ms, which declined only slightly within the subsequent 900 ms (Fig. 5*C*). This overshoot was not observed in atrial myocytes. After 100 ms at −100 mV, I_{peak} had recovered to 96 ± 1% of its amplitude in the conditioning pulse in atrial myocytes (6 cells, 5 hearts), and to 124 ± 7% in ventricular myocytes (7 cells, 4 hearts, $P < 0{\cdot}01$). Time constants (τ_r) were obtained by fitting exponential equations (for formula see legend to Fig. 5) to the data points. Component *a* described the initial rise in values for both cell groups, whereas component *b* was used to describe the decline in overshoot in ventricular myocytes only. The values of τ_{ra} were 55·5 ± 8·1 ms in atrial myocytes and 24·0 ± 1·6 ms in ventricular myocytes ($P < 0{\cdot}01$). The fit to the data for ventricular myocytes was improved by inclusion of component *b*; however, the value obtained for τ_{rb} was 24 513 ± 8995 ms, which has little meaning considering the recovery intervals tested (up to 1000 ms).

Steady-state inactivation of outward current

In atrial myocytes following conditioning pulses negative to −50 mV, the outward current in the test pulse activated and inactivated rapidly with no change in peak current amplitude (Fig. 6*A*). At conditioning potentials between −50 and −20 mV, the amplitude of the inactivating current in the test pulse decreased. Following a conditioning potential of −20 mV, outward current clearly activated more slowly, and hardly inactivated within the 300 ms test

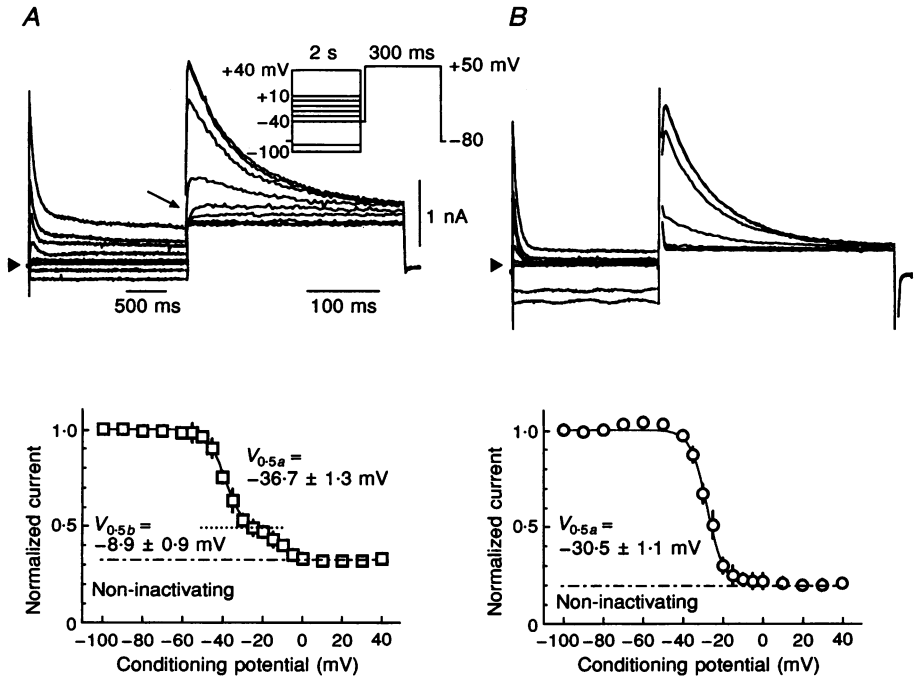

Figure 6. Steady-state inactivation of outward current of human myocytes

A, top: current recordings from an atrial myocyte. Arrowhead, zero current level; cell capacitance was 125 pF. Clamp protocol (inset): holding potential, −80 mV; 2 s conditioning clamp steps at potentials between −100 and +40 mV; a 15 ms clamp step to −40 mV; 300 ms test pulses to +50 mV; frequency, 0·2 Hz. The arrow demonstrates the current recorded in the test pulse following a conditioning potential of −20 mV. Bottom: mean steady-state inactivation curve for 29 atrial myocytes (15 hearts). Ordinate: absolute amplitude of the peak current elicited in the test pulse normalized to the peak current following a conditioning potential at −100 mV (1·0). Abscissa: membrane potential of the conditioning pulse. Two conditioning potential ranges can be clearly seen in which a clear reduction in outward current in the test pulse occurred. The equation $I(V) = a/(1 + \exp(V - V_{0·5a})/k_a) + b/(1 + \exp(V - V_{0·5b})/k_b) + c$, where $I(V)$ was the normalized peak current of the test pulse following the conditioning potential V, $V_{0·5}$ was the potential for half-maximal inactivation for the components *a* and *b*, *k* was the slope factor for each component and *c* was a variable to accommodate the non-inactivating current component. *B*, top: current recording from a ventricular myocyte. Scaling and layout as in *A*; cell capacitance was 302 pF. Bottom: mean steady-state inactivation curve for 26 ventricular cells (7 hearts), layout and normalization as for atrial myocytes. Only a single conditioning potential range was seen in which peak current amplitude in the test pulse was reduced. The equation $I(V) = a/(1 + \exp(V - V_{0·5a})/k_a) + c$ was fitted to the data; variables have identical meaning as for atrial myocytes.

pulse (see arrow in Fig. 6A). With conditioning potentials positive to −20 mV, the amplitude of outward current in the test pulse decreased further. A small fraction of current showed no inactivation at all. To construct steady-state inactivation curves, the absolute maximum amplitude of the current in the test pulse (I_{peak}) was normalized to the amplitude following the conditioning step at −100 mV, and plotted against the membrane potential of the conditioning pulse. In twenty-nine of thirty-six atrial cells (14 hearts), a biphasic potential dependence of inactivation of I_{peak} was observed, so that the steady-state inactivation curve was best described using the sum of two Boltzmann equations (Fig. 6A). Component *a* represents the rapidly inactivating current component, and component *b* the slowly inactivating component seen in the test pulse. The potentials of half-maximum inactivation were −36·7 ± 1·3 mV ($V_{0.5a}$) and −8·9 ± 0·9 mV ($V_{0.5b}$). The respective slope (*k*) values were 3·8 ± 0·2 and 3·5 ± 0·2 mV. Component *a* contributed 50 ± 3% and component *b* 16 ± 1% of I_{peak}, while 34 ± 2% of outward current did not inactivate at all. Thus outward current of human atrial myocytes consists of two distinct, inactivating current components and a third non-inactivating component.

In ventricular myocytes, the peak current amplitude in the test pulse slightly increased at conditioning potentials between −100 and −50 mV, before decreasing with conditioning potentials positive to −40 mV (Fig. 6B). The steady-state inactivation curve was best described using a single Boltzmann function; the corresponding values were: $V_{0.5}$, −30·5 ± 1·1 mV; *k*, 4·2 ± 0·2 mV (26 cells, 7 hearts). The inactivating component contributed 82 ± 2% to the total current and the non-inactivating component contributed 18 ± 2%. The $V_{0.5}$ for ventricular myocytes was significantly positive to the $V_{0.5}$ for the rapidly inactivating component (*a*) of atrial myocytes ($P < 0.01$).

Kinetic separation of the two inactivating current components in atrial myocytes

In atrial myocytes, the current responsible for component *b* of the steady-state inactivation curve could be isolated from that for component *a* by using a 1000 ms prepulse to −20 mV, during which component *a* should completely inactivate. This protocol revealed a rapidly activating outward current that inactivated only slightly within the 300 ms test pulse (sustained outward current or I_{so}, Fig. 7A).

I_{so} in atrial myocytes but not ventricular myocytes

A prominent I_{so} was seen in atrial myocytes (Fig. 7A) and the current–voltage relationship for 114 atrial myocytes is depicted in Fig. 7C. At +40 mV, the absolute current density was 5·1 ± 0·3 pA pF^{-1} for peak I_{so} and 4·7 ± 0·2 pA pF^{-1} for late I_{so} (114 cells, 32 hearts). Inactivation was

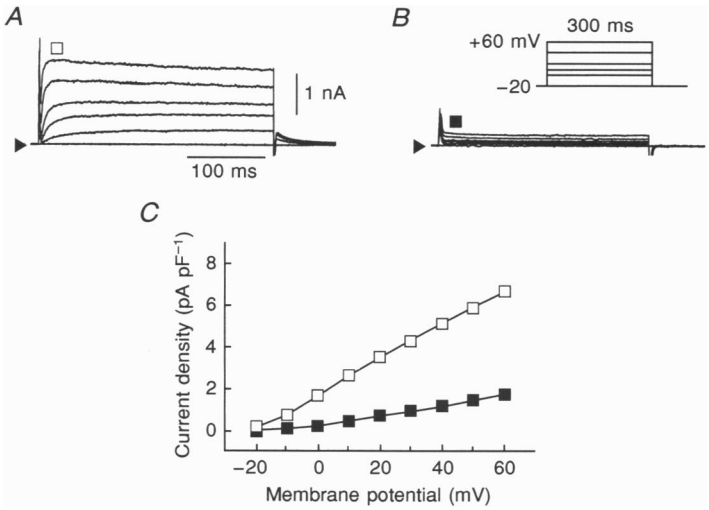

Figure 7. Activation of I_{so} of human myocytes

A, current recording of typical I_{so} in an atrial myocyte. Cell capacitance was 125 pF; scaling as indicated; arrowhead represents zero current level; symbols show times for current measurement. Clamp protocol (inset in *B*): holding potential, −20 mV; test pulses of 300 ms duration to potentials between −20 and +60 mV (10 mV increments; frequency, 0·2 Hz). Between test pulses, a 500 ms clamp step to −100 mV was used to ensure reactivation of all currents; this was followed by a 1000 ms preconditioning pulse at −20 mV to inactivate I_{to} and I_{Na} before the subsequent test pulse. Tail currents were measured at −20 mV. *B*, recording of outward current of a ventricular myocyte activated when using the same protocol as in *A*. Cell capacitance was 283 pF; scaling and layout as in *A*. *C*, current–voltage relationships for the peak outward current of both atrial myocytes (□) and ventricular myocytes (■). Ordinate: mean current density, S.E.M. are within the symbol size, $n = 114$ cells (32 hearts) for atrium and 27 cells (10 hearts) for ventricle. Abscissa: membrane potential of the test pulse.

seen at test potentials positive to +20 mV only and amounted to 7 ± 1 % of I_{peak} at +40 mV. In only sixty-one atrial cells were we able to describe the time course of I_{so} inactivation at +40 mV. The time course of inactivation for these cells was mono-exponential, the time constant being 865 ± 173 ms. The inactivation time course in the remaining fifty-three cells was too slow to be resolved within the 300 ms test pulse.

In contrast to atrial cells, no I_{so}-like current was seen in ventricular cells (Fig. 7*B*). The activation kinetics of outward current with depolarization following conditioning pulses to −20 mV could not be separated from capacitive transients, and the current decayed only slightly during the initial 50 ms of the test pulses. The current–voltage relationship for this current in ventricular myocytes is depicted in Fig. 7*C*. At +40 mV, the current density was 1·2 ± 0·2 pA pF^{-1} for peak current and 0·9 ± 0·1 pA pF^{-1} for late current (27 cells, 10 hearts).

Pharmacological separation of I_{to} and I_{so} in atrial myocytes

Confirmation that I_{so} and I_{to} are completely separate currents necessitates not only a kinetic but also a pharmacological differentiation. We have therefore tested the effects of several K^+ channel blockers, and of substitution of extracellular Na^+, on both currents in atrial myocytes.

4-Aminopyridine. Apkon & Nerbonne (1991) have differentiated between two components of outward current in rat ventricular myocytes using 4-AP. Therefore, the effects of 4-AP on outward currents of human atrial myocytes were tested for concentrations between 5 μM and 10 mM. 4-AP reduced I_{so} at concentrations markedly lower than that required to reduce I_{to} (Fig. 8*A* and *B*). To characterize the concentration dependence of block, the absolute I_{so} current amplitude 20 ms after initiation of a test pulse to +40 mV following a conditioning step to −20 mV was measured and normalized to the control amplitude (1·0) and plotted against the logarithm of the corresponding 4-AP concentration. The amplitude of I_{to} during a test pulse to +40 mV (defined as the transient component of the difference current of total current minus I_{so}) was normalized as for I_{so}. A sigmoidal function was fitted to the data points (Fig. 8). The concentration of half-maximum inhibition (IC_{50}) by 4-AP was 5·8 μM for I_{so} and 1·0 mM for I_{to}. The greater sensitivity of I_{so} to 4-AP block confirms that I_{to} and I_{so} are indeed two individual currents. The 'shoulder' seen when using the slowly depolarizing ramp protocol (Fig. 2) was also sensitive to low concentrations of 4-AP (data not shown), suggesting that this 'shoulder' was due to activation of I_{so}.

4-AP also reduced I_{to} peak current amplitude in ventricular myocytes. The amplitude of I_{late}, however, was not significantly influenced, even at very high (10 mM) concentrations. Interestingly, 4-AP was less potent at blocking I_{to} in ventricular myocytes than in atrial myocytes. In ventricular myocytes, 1 mM 4-AP reduced I_{to}

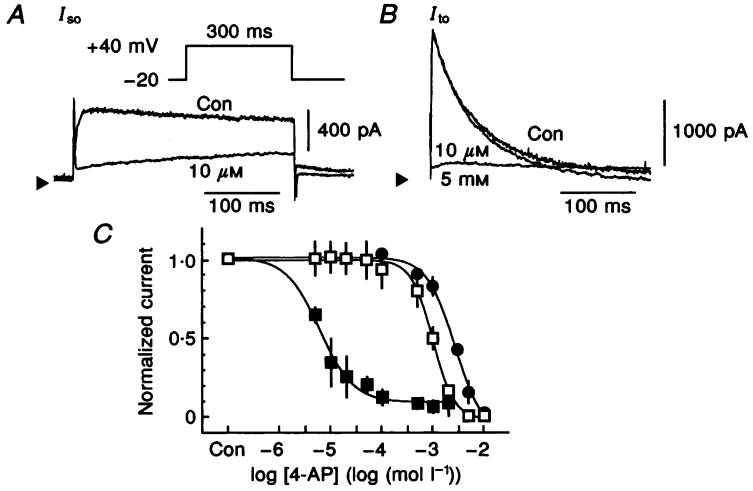

Figure 8. Differential effects of 4-aminopyridine on I_{to} and I_{so} of human atrial myocytes

A, effect of 4-AP (10 μM) on I_{so} activated by a 300 ms test pulse to +40 mV from a holding potential of −20 mV. Scaling and protocol as indicated; arrowheads show zero current level; Con, control recording. Cell capacitance was 125 pF. *B*, effect of 4-AP (10 μM and 5 mM) on I_{to} at +40 mV obtained by subtracting I_{so} from the total outward current. Scaling as indicated; current recordings are from the same cell as in *A*. Please note the greater effect of 10 μM 4-AP on I_{so} than on I_{to}. *C*, concentration–response curves for 4-AP blockade of I_{so} (■) and I_{to} (□) of human atrial myocytes, and of I_{to} in human ventricular myocytes (●); $n = 4$–5. Ordinate: current amplitudes in the presence of 4-AP normalized to the current amplitude under control conditions. Abscissa: concentrations of 4-AP expressed as log (mol l^{-1}); Con, control. The sigmoidal function $I = 1/(1 + (10^{pD_2}/10^C)^{n_H})$ where I is the normalized current amplitude in the presence of 4-AP, C is the logarithm of the concentration of 4-AP, pD_2 is the logarithm of the concentration for half-maximal block and n_H is the 'Hill' slope.

amplitude by 18 ± 6%, whereas in atrial myocytes, the same concentration reduced I_{to} amplitude by 51 ± 3% ($P < 0.01$). To characterize the concentration dependence of block of ventricular I_{to}, the amplitude of I_{peak} for a test pulse at +40 mV in the presence of 4-AP was normalized to I_{peak} amplitude under control conditions (Fig. 8*C*). The IC_{50} value for reduction in I_{peak} was 2·7 mM.

Tetraethylammonium. TEA blocks an I_{so}-like current without influencing an I_{to}-like current in rat ventricular myocytes (Apkon & Nerbonne, 1991). In human atrial myocytes, TEA (20 mM) did not significantly influence outward currents (Fig. 9*A*). Peak total outward current (+40 mV, 22 °C) was not significantly altered (control, 13·2 ± 2·0 pA pF^{-1}; TEA, 13·5 ± 2·2 pA pF^{-1}; $n = 4$). Late current was also not significantly reduced (control, 8·4 ± 2·0 pA pF^{-1}; TEA, 7·8 ± 2·0 pA pF^{-1}). TEA (20 mM) had no significant effect on outward currents of human ventricular myocytes. Peak current amplitude at +40 mV was not significantly altered with 5 min exposure (control, 4·0 ± 0·4 pA pF^{-1}; TEA, 4·1 ± 0·7 pA pF^{-1}; $n = 4$). I_{late} was also not affected (control, 1·0 ± 0·2 pA pF^{-1}; TEA, 1·0 ± 0·2 pA pF^{-1}).

Dendrotoxin. DTX selectively blocks some families of voltage-dependent K^+ channels (for review, see Strong,

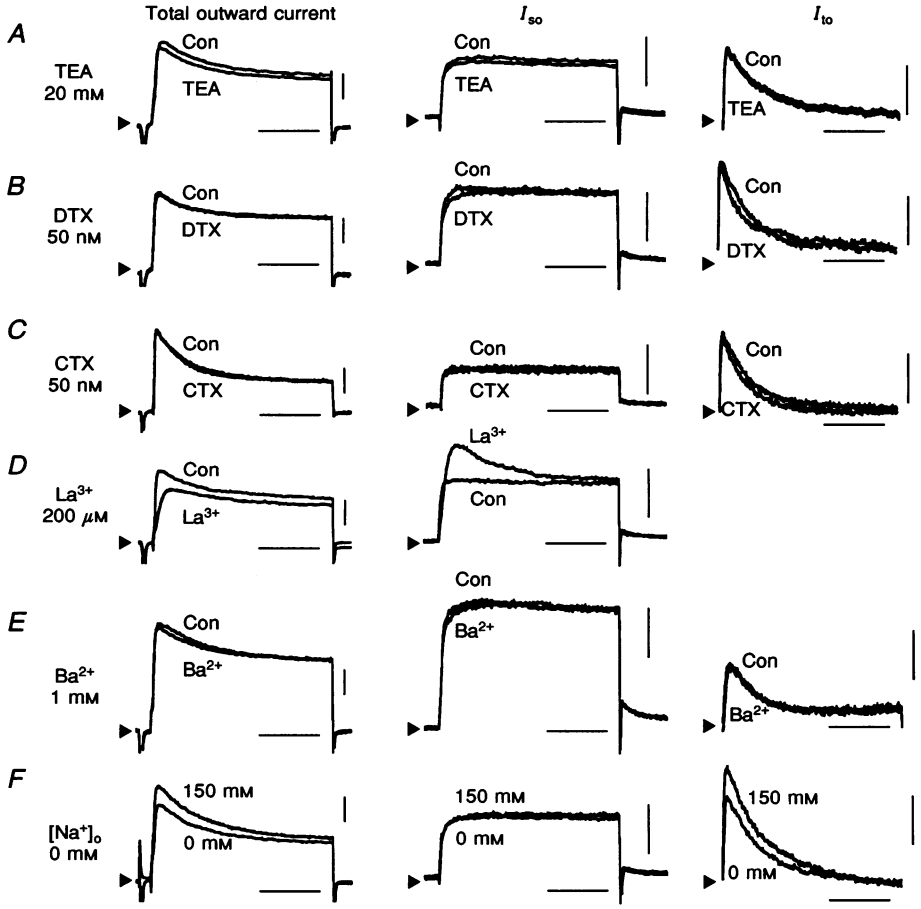

Figure 9. The effect of K^+ channel blockers and replacement of extracellular Na^+ on outward currents of human atrial myocytes at 22 °C

I_{to} is defined as the transient component of the difference current of total outward current minus I_{so}. Current recordings for test pulses at +40 mV are shown. Current scale bar, 500 pA (please note the amplification is twice as large for I_{so} and I_{to} as for the total outward current); time scale bar, 100 ms. *A*, effects of 20 mM TEA on total outward current (left), I_{so} (middle) and I_{to} (right). No significant influence was seen. *B*, effects of 50 nM DTX on the atrial outward currents, layout as in *A*. Outward currents were not significantly reduced. *C*, effects of 50 nM CTX on atrial outward currents, layout as in *A*. No significant reduction in outward currents was detected. *D*, effects of 200 μM lanthanum (La^{3+}) on atrial outward currents, layout as in *A*. No marked block of I_{so} was evident. Difference currents for I_{to} are not shown as I_{to} and I_{so} could not be separated with conditioning steps to −20 mV due to the La^{3+}-induced shifts in I_{to} steady-state inactivation. *E*, effects of 1 mM barium (Ba^{2+}) on atrial outward currents, layout as in *A*. Outward currents were not significantly blocked. *F*, effects of replacement of extracellular Na^+ with *N*-methyl-D-glucamine on atrial outward currents, layout as in *A*. Peak outward current was significantly reduced.

1990). DTX (50 nM) had no significant effect on outward currents of human atrial myocytes (Fig. 9*B*). Peak total outward current amplitude during a test pulse to +40 mV was not significantly reduced (control, 5·3 ± 0·7 pA pF^{-1}; DTX, 5·2 ± 0·6 pA pF^{-1}; $n = 3$). Late total outward current was 3·2 ± 0·7 before, and 3·1 ± 0·9 pA pF^{-1} following exposure to 50 nM DTX (not significant (n.s.)).

Charybdotoxin. CTX is a selective blocker of K^+ channels, in particular those dependent on the intracellular [Ca^{2+}] (for review, see Strong, 1990). CTX (50 nM) had no significant effect on outward currents in human atrial myocytes (Fig. 9*C*). Peak total outward current of four atrial myocytes during a test pulse to +40 mV was not changed (control, 16·4 ± 3·0 pA pF^{-1}; CTX, 16·4 ± 3·5 pA pF^{-1}). Late total outward current was also not significantly altered (control, 10·9 ± 2·6 pA pF^{-1}; CTX, 11·3 ± 2·6 pA pF^{-1}).

Lanthanum. The rapidly activating component of the delayed rectifier current (I_{Kr}) in guinea-pig ventricular myocytes is selectively blocked by lanthanum (Sanguinetti & Jurkiewicz, 1990). The effect of $LaCl_3$ (200 μM) on outward currents of human atrial myocytes was complex (Fig. 9*D*). Exposure to $LaCl_3$ shifted the steady-state inactivation curve of I_{to} to positive potentials, such that I_{to} and I_{so} could not be separated with conditioning steps even to +30 mV. However, I_{late} and tail current amplitude following a conditioning pulse to −20 mV was not significantly reduced by $LaCl_3$ (at +40 mV; control I_{late}, 7·6 ± 1·3 pA pF^{-1}; $LaCl_3$ I_{late}, 8·3 ± 1·5 pA pF^{-1}; $n = 4$, Fig. 9*D*), indicating that I_{so} was probably not blocked.

Barium. Barium blocks a second rapidly activating, non-inactivating outward current, I_{Kp}, in guinea-pig ventricular myocytes (Backx & Marban, 1993). The outward currents of four human atrial myocytes were not significantly altered following exposure to 1 mM $BaCl_2$ (Fig. 9*E*). The peak total outward current amplitude at +40 mV was 8·8 ± 1·7 pA pF^{-1} before and 8·7 ± 1·7 pA pF^{-1} after exposure to $BaCl_2$ (n.s.). Late total outward current was also not significantly influenced (control, 6·5 ± 1·8 pA pF^{-1}; barium, 6·4 ± 1·7 pA pF^{-1}).

Replacement of extracellular Na^+. Dukes & Morad (1991) have reported that replacement of Na^+ in the bath solution shifts the steady-state inactivation of I_{to} in rat ventricular myocytes to more negative potentials. Such a shift in steady-state inactivation of I_{to} but not of I_{so} in human atrial myocytes would facilitate separation of these two components. We have therefore tested the effects of replacing extracellular Na^+ with *N*-methyl-D-glucamine in four atrial myocytes.

Replacement of extracellular Na^+ significantly reduced peak total outward current from 8·6 ± 1·5 to 7·1 ± 1·1 pA pF^{-1} ($n = 4$, $P = 0·03$) without significantly reducing the late current (150 mM, 4·7 ± 0·4 pA pF^{-1}; 0 mM, 4·0 ± 0·4 pA pF^{-1}; Fig. 9*F*). In 150 mM Na^+-containing bath solution, changing the holding potential to −60 mV did not induce a significant reduction in outward current, indicating that the observed effects of Na^+ replacement were not secondary to the diminished I_{Na} during the prepulse to −40 mV.

The significant reduction of peak total outward current suggests that an effect on I_{to} but not I_{so} was responsible, which was confirmed following separation of I_{so} from I_{to} (Fig. 9*F*). I_{so} peak and late current density at +40 mV were not affected following replacement of extracellular Na^+. Peak I_{so} was 3·5 ± 0·5 pA pF^{-1} before, and 3·0 ± 0·5 pA pF^{-1} following Na^+ replacement ($n = 4$). Similarly, late I_{so} was not significantly reduced (150 mM, 3·4 ± 0·5 pA pF^{-1}; 0 mM, 3·0 ± 0·3 pA pF^{-1}). In contrast, the amplitude of I_{to} at +40 mV was significantly reduced from 4·2 ± 0·7 to 3·1 ± 0·7 pA pF^{-1} following Na^+ replacement ($P = 0·05$).

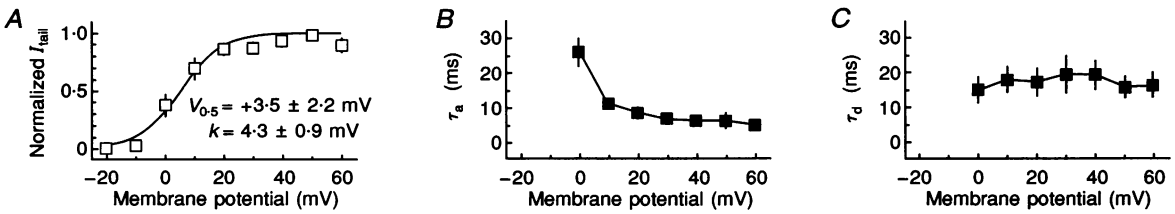

Figure 10. Further characterization of I_{so} of human atrial myocytes

A, potential dependence of activation calculated from tail currents at −20 mV following activating clamp steps of 60 ms duration. Ordinate: amplitude of the tail current (I_{tail}) was normalized to tail current amplitude following an activating step to +50 mV; abscissa: potential of the activating clamp step. Data are expressed as means ± S.E.M. from 5 cells. The equation $I(V) = 1/(1 + \exp((V - V_{0·5})/k))$ was fitted to the data, where $I(V)$ is the normalized tail current following an activating potential V, $V_{0·5}$ is the potential for half-maximal activation and k is the slope factor. *B*, potential dependence of the time constant (τ_a) of activation. Capacitive transients and background current were digitally subtracted from the original current recording, as described in Methods. The resulting current tracing was fitted with a mono-exponential function. The values for τ_a (ordinate) were plotted against the potential for activation (abscissa). *C*, potential dependence of the time constant (τ_d) of deactivation. Values for τ_d were obtained by fitting tail current recordings with a mono-exponential equation. The values for τ_d (ordinate) were plotted against the potential for activation (abscissa).

Unlike in rat myocytes (Dukes & Morad, 1991), reduction in I_{to} in human atrial myocytes was not explained by a shift in the steady-state inactivation curve to more negative potentials. Indeed, $V_{0.5}$ for I_{to} inactivation was shifted from -33.7 ± 1.1 to -30.7 ± 1.0 mV ($P = 0.014$). To determine the voltage dependence of activation, I_{to} amplitudes were converted to conductance values by assuming a linear fully activated current–voltage relationship and an experimentally determined reversal potential of −55 mV (Näbauer *et al.* 1993; Wettwer *et al.* 1994). The steady-state activation curves were described with a single Boltzmann equation. The potential for half-maximal activation was shifted from $+13 \pm 4$ mV (150 mM Na^+) to $+25 \pm 6$ mV (0 mM Na^+) with no effect on the slope factor k. This shift in potential dependence of activation can explain the reduced I_{to} amplitude, as the number of channels available for activation at +40 mV is reduced by ~20%. No such shift was observed for I_{so} activation curves; $V_{0.5}$ was -8 ± 2 mV in 150 mM Na^+ and -6 ± 2 mV in 0 mM Na^+, as calculated from tail current amplitudes at −20 mV. Although not providing a means for easier separation of I_{so} and I_{to}, the selective influence of extracellular Na^+ replacement does provide further evidence that two completely individual currents are involved.

Further characterization of the sustained outward current I_{so}

Kinetics of I_{so} activation and deactivation. Voltage dependence of I_{so} activation was investigated in five atrial cells from two hearts by applying 60 ms test pulses between −20 and +60 mV, preceded by 1000 ms conditioning pulses at −20 mV. Tail currents at −20 mV could then be measured before significant inactivation of I_{so} occurred. Steady-state activation curves were constructed by normalizing tail current amplitudes to the maximum amplitude and fitting a single Boltzmann function (Fig. 10*A*). This method of analysis gave values of $+3.5 \pm 2.2$ mV for the potential of half-maximum activation ($V_{0.5}$) and 4.3 ± 0.9 mV for the slope factor k. To obtain the time constants of I_{so} activation (τ_a), the capacitive transients and background currents were subtracted as described in Methods. The resulting current was fitted with a first-order power function. The value of τ_a decreased with more positive test pulse potentials (Fig. 10*B*), such that at +60 mV, peak current was observed within 20 ms. The time course of deactivation at −20 mV was adequately described using a single exponential function and the time constant τ_d (19 ± 4 ms following a clamp step to +40 mV) was not dependent on the potential of the activating clamp step (Fig. 10*C*).

Envelope-of-tails test. In an envelope-of-tails test, currents activated during clamp steps of variable duration (I_{step}) are compared with the deactivating tail current (I_{tail}). If the ratio of I_{tail}/I_{step} is independent of the clamp step duration, it is concluded that a single channel type only contributes to the investigated current. An envelope-of-tails test was performed on I_{so} (7 cells, 5 hearts). Two potentials for activation were chosen in order to test I_{so} at membrane potentials where slow (+60 mV) and no inactivation (+20 mV) were observed during a 300 ms test

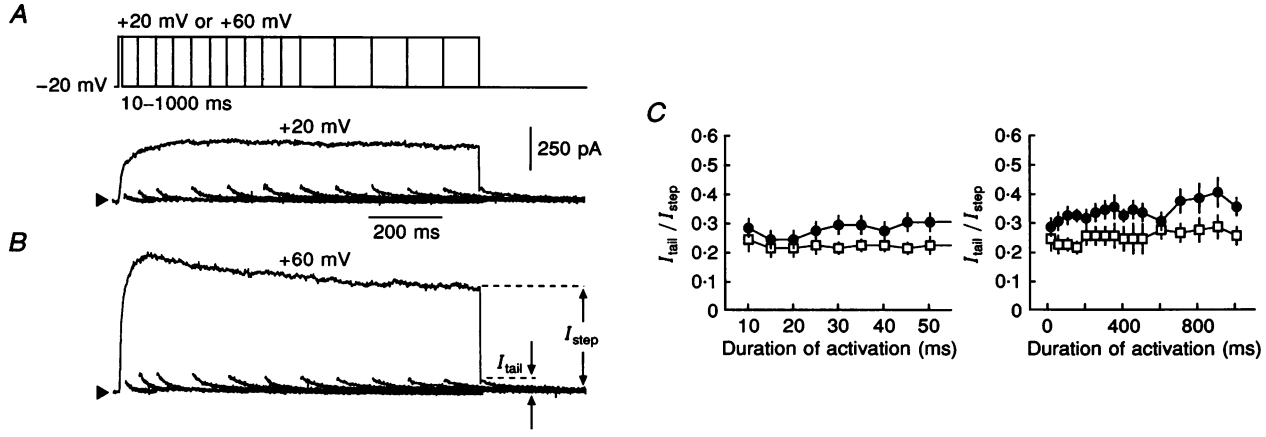

Figure 11. Envelope-of-tails test for I_{so} of human atrial myocytes

A, record of current activated when performing an envelope-of-tails test for an activating step to +20 mV. Scaling as indicated; arrowheads represent zero current level; cell capacitance was 125 pF. Clamp protocol (inset): holding potential of −100 mV to ensure reactivation of all currents; a 1000 ms preconditioning pulse at −20 mV to inactivate I_{to} and I_{Na}; test pulses of increasing duration (from 10 to 1000 ms) at potentials of +20 or +60 mV; tail currents were measured at −20 mV; frequency, 0·2 Hz. *B*, record of current activated when performing an envelope-of-tails test for an activating step to +60 mV. Scaling and protocol as indicated in *A*, same cell as in *A*. *C*, time dependence of the quotient of tail current amplitude (I_{tail}) and the amplitude of the current activated during activating clamp steps (I_{step}) to +20 mV (●) and +60 mV (□). Ordinate: amplitude of I_{tail} expressed as a fraction of I_{step} for 7 cells (6 hearts). Abscissa: duration of I_{step}. Left: data obtained with activating pulses up to 50 ms duration; right: data obtained with activating pulses from 10 to 1000 ms duration.

pulse (Fig. 11*A* and *B*). Tail currents were measured at −20 mV. When activating outward current by clamp steps to +20 or +60 mV, the ratio of I_{tail}/I_{step} was not dependent on the duration of the activating pulse (Fig. 11*C*).

I_{so} at physiological temperature. Characterization of current kinetics at physiological temperature is necessary in order to gain a better understanding of the role of that current during an action potential *in vivo*. When testing the effect of raising the experimental temperature to 37 °C on I_{so}, we have increased the duration of the test pulses to 4 s to improve resolution of the slow inactivation process. At 22 °C I_{so} activated rapidly and inactivated slowly during the 4 s test pulse (Fig. 12*A*). The current densities of I_{peak} and I_{late} were 4·5 ± 0·8 and 2·4 ± 0·3 pA pF^{-1}, respectively ($n = 4$). The inactivation time course was mono-exponential and the corresponding time constant was 2163 ± 402 ms ($n = 4$). Raising the bath temperature accelerated the rate of I_{so} activation and significantly increased the current density of I_{peak} (6·5 ± 0·6 pA pF^{-1}, $P < 0·01$). The inactivation time course was markedly accelerated (Fig. 12*A*), so that the current density of I_{late} was significantly smaller than at 22 °C (2·0 ± 0·2 pA pF^{-1}, $P = 0·01$) and no tail current was observed when returning the membrane potential to −20 mV. The time course of I_{so} inactivation at 37 °C became double exponential and the corresponding time constants were 359 ± 46 and 1918 ± 342 ms.

Further characterization of the transient outward current I_{to}

Potential dependence of I_{to} activation. To characterize the potential dependence of activation of atrial and ventricular I_{to}, the inactivating components of the total outward current (i.e. $I_{peak} - I_{late}$) during a 300 ms test pulse were converted to conductance values by assuming a linear fully activated current–voltage relationship and an experimentally determined reversal potential of −55 mV (Näbauer *et al.* 1993; Wettwer *et al.* 1994). The steady-state activation curves were well described with a single Boltzmann equation. The potentials for half-maximum activation ($V_{0·5}$) of I_{to} were not significantly different between 145 atrial and thirty-nine ventricular cells (+11·8 ± 1·0 and +10·5 ± 1·3 mV, respectively). The values for the slope factor (k) were also not different (atrium, 11·2 ± 0·4 mV; ventricle, 11·2 ± 0·4 mV).

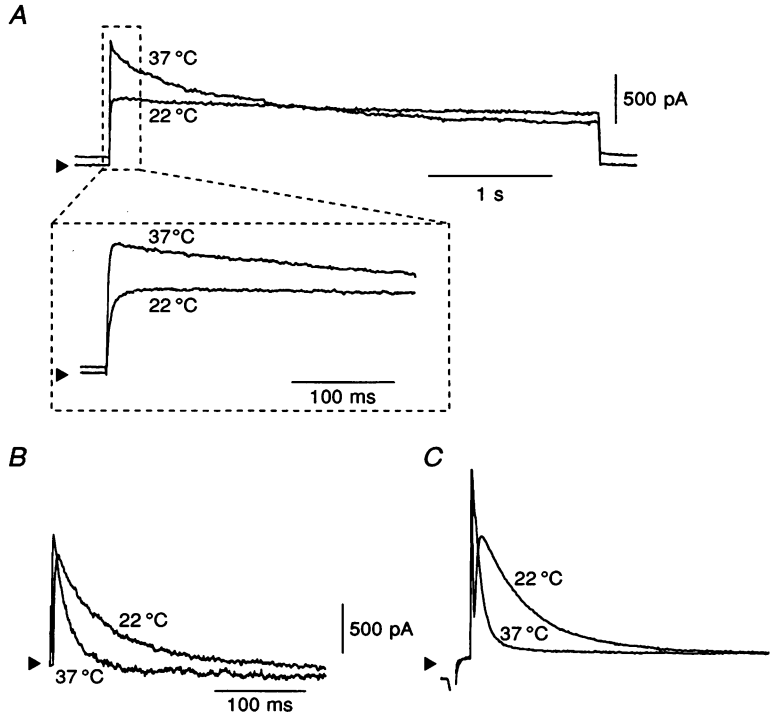

Figure 12. Original recordings of I_{so} and I_{to} at room and physiological temperature

A, original recordings of I_{so}. Arrowheads show zero current level; cell capacitance was 186 pF. Clamp protocol: holding potential, −20 mV; test pulses of 4 s duration to +40 mV. Top: current recording for the complete 4 s test pulse; bottom: current recording expanded to show the first 300 ms of the test pulse. Note the different time scales. *B*, original recording of I_{to} at +40 mV from an atrial myocyte at 22 and 37 °C. I_{to} was defined as the difference between the total outward current and I_{so}. Arrowhead shows zero current level; cell capacitance was 186 pF. *C*, original recording of I_{to} at +40 mV from a ventricular myocyte at 22 and 37 °C. Clamp protocol: holding potential, −80 mV; 25 ms clamp step to −40 mV; 300 ms test step to +40 mV. Layout and scaling as in *B*; cell capacitance was 282 pF.

I_{to} at physiological temperature. Original recordings of atrial and ventricular I_{to} at 22 and 37 °C are shown in Fig. 12*B* and *C*. At 22 °C, I_{to} activation was rapid and the amplitudes ($I_{peak} - I_{late}$) of I_{to} were $4{\cdot}9 \pm 0{\cdot}5$ pA pF^{-1} (atrium, $n = 4$) and $4{\cdot}0 \pm 0{\cdot}9$ pA pF^{-1} (ventricle, $n = 6$). The time constant of inactivation at +40 mV was 58 ± 5 ms for atrial I_{to} and 61 ± 2 ms for ventricular I_{to}. In atrial myocytes, raising the bath temperature to 37 °C accelerated the rate of I_{to} activation, without significantly increasing I_{to} amplitude ($6{\cdot}2 \pm 0{\cdot}7$ pA pF^{-1}). In ventricular myocytes, the speed of I_{to} activation became too rapid to separate peak I_{to} amplitude from the capacitive transient. The inactivation of I_{to} was also markedly accelerated in both cell types, the time constants being reduced to 12 ± 2 ms (atrium) and 22 ± 4 ms (ventricle).

DISCUSSION

The outward current of human atrial myocytes at room temperature consists of three distinct current components: a rapidly activating and inactivating current (I_{to}), a rapidly activating but slowly inactivating current (I_{so}) and a non-characterized background current. I_{to} and I_{so} could be distinguished by differences in inactivation kinetics and sensitivity to 4-AP. I_{to} and background current, but not I_{so}, were observed in human ventricular myocytes. Slight but significant differences in the properties of I_{to} were, however, detected between atrium and ventricle.

Potential limitations due to cell isolation

The limited number of cells investigated from a single tissue sample were selected by the following criteria: rod shape, clear cross striations, seal resistance (> 1 GΩ) and relative small size in order to ensure high quality of voltage control. This raises the question whether the myocytes studied were truly representative for the source of tissue. It is conceivable that only non-diseased myocytes, but not cells representative for diseased myocardium, survived the isolation procedures. Evidence against such a bias was, however, provided by the demonstration of differences in outward currents of ventricular myocytes obtained from failing and non-failing hearts (Beuckelmann *et al.* 1993; Wettwer *et al.* 1994). In the current study, results obtained for subepicardial myocytes were used because of the pronounced amplitude of I_{to} in these cells (Wettwer *et al.* 1994). Despite the potential limitations, characterization of the electrophysiological properties of human myocytes is important due to the limitations of extrapolating animal models to the human.

Differences between atrial and ventricular myocytes

Cell size and resting membrane potential. The cell capacitance was significantly smaller for atrial than for ventricular myocytes. In many mammalian species, atrial myocytes are of smaller size than ventricular myocytes and possess less developed transverse tubules (Canale, Campbell, Smolich & Campbell, 1986). Similar morphological differences in human hearts could account for the different values in cell capacitance. The greater size of human ventricular myocytes may also represent ventricular remodelling and hypertrophy in the advanced stages of heart failure (Grajek, Lesiak, Pyda, Zajac, Paradowski & Kaczmarek, 1993).

The measured resting membrane potential was significantly more positive in atrial than in ventricular myocytes, though both groups were relatively depolarized. This depolarization raises the question of possible cell damage due to ischaemic periods during surgical procedure, transport to the laboratory, isolation procedure and experimentation. To estimate depolarization due to leak currents through the electrode/cell membrane seal, the corrected membrane potential (V_{cM}) was calculated from the seal resistance (R_{seal}), the membrane resistance (R_M) and the experimentally measured membrane potential (V_{mM}) for cells in which R_M was determined. It follows that $V_{cM} = V_{mM} \times R_M/R_{seal} + V_{mM}$, if R_{seal} is considered to be in series with R_M (Schneider & Chandler, 1976). The corrected resting membrane potentials for both cell groups were not significantly different between atrial (-63 ± 2 mV; $n = 54$) and ventricular myocytes (-65 ± 2 mV; $n = 20$).

Depolarized cells have also been reported for multicellular human preparations, with significantly more positive membrane potential in atrial myocytes from diseased than non-diseased hearts (Ten Eick & Singer, 1979) or regions of depolarized and normal cells within the same ventricular preparation (McCollough, Chua, Rasmussen, Ten Eick & Singer, 1990). The relative depolarization of atrial and ventricular myocytes in our study would therefore appear to be a biological phenomenon amplified by experimental artifacts, in particular the low seal resistance when compared with membrane resistance.

The inward rectifier (I_{K1}) is smaller in atrial myocytes than ventricular myocytes. The net inwardly directed current at the beginning of the slowly depolarizing ramp (−100 mV) was significantly smaller in atrial myocytes than in ventricular myocytes. Inward current at this potential in human ventricular myocytes represents I_{K1}, as it is completely blocked with 1 mM barium (Beuckelmann *et al.* 1993). According to Thuringer, Lauribe & Escande (1992), the inward current at −100 mV in human atrial myocytes is the sum of I_{K1} and the pacemaker current I_f. In our experiments, 1 mM barium reduced the inward current at −100 mV by approximately 60% (G. J. Amos, unpublished observations); however, we did not observe any I_f-like current in any atrial myocyte in this study. Therefore, the identification of the net inward current at −100 mV with I_{K1} in atrial myocytes would, if anything, overestimate the I_{K1} amplitude, leading to the conclusion that I_{K1} is smaller in atrial than in ventricular myocytes. The smaller I_{K1} of atrial myocytes contributes to the high membrane resistance when compared with ventricular myocytes.

I_{so} present in atrium but not ventricle. The large late outward current of human atrial myocytes resulted from a distinct slowly inactivating current I_{so} underlying the rapidly inactivating I_{to}. Evidence supporting the presence of such a current in atrial cells included: (i) an outwardly directed 'shoulder' in current at positive membrane potentials when using slowly depolarizing ramp pulses, (ii) a rapid and a slow component of outward current inactivation, (iii) a biphasic potential dependence of steady-state inactivation, (iv) a rapidly activating, slowly inactivating outward current following prepulses to −20 mV, (v) 60-fold greater sensitivity of I_{so} to 4-AP block than I_{to}, and (vi) a shift in I_{to} but not I_{so} activation kinetics following replacement of extracellular Na^+. No evidence for I_{so} was found in ventricular myocytes. I_{so} was blocked by intracellular Cs^+ and therefore is probably a K^+ current. As an envelope-of-tails test was satisfied, the slow inactivation of I_{so} was due to changes in the membrane conductance, and not to accumulation or depletion of K^+ ions near the surface of the membrane.

The rapid activation and relatively slow inactivation of I_{so} (even at physiological temperature) would allow this current to participate in both early and late phases of atrial action potential repolarization. Low concentrations of 4-AP, which selectively block I_{so}, have been shown to prolong the action potential at all phases of repolarization in human atrial myocytes (Wang *et al.* 1993*b*). Therefore, by prolonging atrial refractory period, blockers of this current would provide a possible mechanism for the pharmacological handling of supraventricular arrhythmias. Selective blockers of I_{so} would prolong the refractory period of atrium only, thus reducing the risk of life-threatening ventricular arrhythmias such as torsade de pointes.

The properties of I_{so} are similar to those of the recently described slowly inactivating K^+ current, I_{sus}, in human atrial myocytes (Wang *et al.* 1993*b*). I_{so} inactivated to a greater extent (by 28 ± 5% after 1000 ms at +60 mV) than I_{sus} (by only 19 ± 2% after 2000 ms). I_{so} was also more sensitive to 4-AP block than I_{sus}: half-maximum block of I_{so} occurred at 8 μM and of I_{sus} at 49 μM. This difference in potency of 4-AP may be due to the activation protocols, since the blocking effect of 4-AP is potential dependent, being greatest at membrane potentials close to resting potential and decreasing with depolarization (Castle & Slawsky, 1993). This results in recovery from block during the depolarizing conditioning clamp step required for I_{to} inactivation. Unblock of the I_{so} channel should be larger at strongly positive conditioning potentials, i.e. +50 mV (Wang *et al.* 1993*b*) *versus* −20 mV (this study), resulting in an apparent lower affinity of 4-AP. In conclusion, despite the differences in properties of I_{so} and I_{sus}, these two currents probably involve the same channel.

In animal models, several K^+ currents with similar kinetic properties to I_{so} have been described. Backx & Marban (1993) reported the presence of such a current in guinea-pig ventricular myocytes (I_{Kp}), which was blocked with 1 mM $BaCl_2$ and therefore is not equivalent to I_{so}. A second rapidly activating, non-inactivating K^+ current I_{Kr} has been reported in guinea-pig ventricular myocytes (Sanguinetti & Jurkiewicz, 1990). However, unlike I_{so}, I_{Kr} is sensitive to La^{3+} and shows marked inward rectification at positive membrane potentials. The insensitivity of I_{so} (G. J. Amos, unpublished observations) to the selective I_{Kr} blocker almokalant provides further evidence for non-identity of the two currents. Recently, a human K^+ channel gene expressing channels with I_{Kr} properties has been cloned and characterized (Sanguinetti, Jiang, Curran & Keating, 1995). An I_{Kr}-like current, however, could not be detected in isolated human myocytes for unknown reasons. In rat ventricle, Apkon & Nerbonne (1991) have reported a rapidly activating, slowly inactivating K^+ current sensitive to TEA but not to 4-AP and therefore not identical to I_{so}. Boyle & Nerbonne (1992) have also reported a rapidly activating, slowly inactivating K^+ current in rat atrial myocytes. This current was sensitive to 4-AP in millimolar concentrations, however, and inactivated at more negative membrane potentials (despite 5 mM extracellular $CoCl_2$) than I_{so} and is therefore similar but not identical to I_{so}. Thus an equivalent current to I_{so} in myocardial preparations from animal models remains to be found, demonstrating the value of investigations using human myocardium.

Differences in I_{to} between atrial and ventricular myocytes. A rapidly activating and inactivating outward current (I_{to}) of similar density (when $I_{peak} - I_{late}$ of the total outward current is considered representative) was observed in both atrial and ventricular myocytes. I_{to} was blocked by intracellular Cs^+ and therefore is probably a K^+ current, though the relatively positive reversal potential indicates that the underlying channels are not completely K^+ selective (Näbauer *et al.* 1993; Wettwer *et al.* 1994). Significant differences in I_{to} properties between atrial and ventricular cells were, however, observed. The time course of I_{to} inactivation was slightly faster and steady-state inactivation occurred at more negative potentials in atrium than in ventricle. Furthermore, the recovery from inactivation was slower and without overshoot in atrial myocytes. In addition, 4-AP was almost three times more potent at blocking atrial than ventricular I_{to}. These differences in I_{to} properties between atrial and ventricular myocytes suggest the underlying channels are similar but not identical in these two cell types. Severity of heart failure is not likely to underlie the different properties of I_{to} since the characteristics of I_{to} are identical in epicardial cells from end-stage failing hearts and from donor hearts (Wettwer *et al.* 1994).

Non-inactivating currents were larger in atrial myocytes than in ventricular myocytes. In both atrial and ventricular cells, outward current at 22 °C did not inactivate completely even during 2 s long, strongly positive conditioning clamp steps. The non-inactivating current was

considerably larger in atrial myocytes than in ventricular myocytes. A large component of this current in atrial myocytes was probably I_{so}, as the 2 s conditioning pulse was not long enough for complete inactivation (τ of inactivation was 1425 ms). The late current density was not significantly different between atrial and ventricular myocytes in the presence of 100 μM 4-AP (G. J. Amos, unpublished observations), supporting this hypothesis. A typical delayed rectifier (I_K) probably did not contribute to this current as TEA had no significant effect on outward currents at 22 °C. Indeed, we found no evidence for I_K in either ventricular or atrial myocytes, even at 37 °C. Investigations demonstrating the existence of this current in both human atrial (Wang *et al.* 1993*a*) and ventricular myocytes (Beuckelmann *et al.* 1993) have been recently published. Both groups reported rapid run-down of this current, especially when using electrodes with large tip diameters. Therefore run-down of I_K may have been so rapid under our conditions that the current quickly disappeared following membrane disruption. The presence of extracellular $CdCl_2$ is not a likely explanation for the absence of I_K, as Cd^{2+} increases the amplitude of I_K in cat ventricular myocytes (Follmer, Lodge, Cullinan & Colatsky, 1992). Thus the reasons for the absence of I_K under our conditions remain unclear.

Following replacement of K^+ with Cs^+ in the pipette solution, an outward current of similar density was observed in both atrial and ventricular myocytes. Only a minor fraction of this current could be non-selective leak current due to electrode seal resistance (at +60 mV, a 2 GΩ seal resistance would produce a leak current of only 30 pA). Chloride conductance probably does not contribute to this current since replacement of extracellular NaCl with $NaSO_3CH_3$ did not significantly reduce outward currents in atrial (Wang *et al.* 1993*b*) or in ventricular myocytes (G. J. Amos, unpublished results). A possible candidate would be currents through non-selective cation channels but this requires further investigation.

Differences in action potential shape. The short action potential duration and plateau at more negative potentials in atrial myocytes indicates a greater domination of outward currents during repolarization. Smaller inward currents such as I_{Ca} in atrial myocytes rather than in ventricular myocytes (Mewes & Ravens, 1994) could amplify outward current domination. I_{Na} probably does not contribute to the effect, as the maximum Na^+ conductance is not different in human atrial and ventricular myocytes in reduced extracellular [Na^+] (Furukawa *et al.* 1995), and no non-inactivating I_{Na} has yet been reported in atrial (Jia *et al.* 1993) or ventricular myocytes (Sakakibara *et al.* 1993). Greater domination of outward current in atrial than in ventricular myocytes is mainly caused by the selective presence of I_{so} in atrial cells, since I_{to} current densities were similar in both types of myocytes and the smaller amplitude of I_{K1} in atrial cells should cause reduction of this difference.

Regional variations in outward currents within atrium or ventricle

The current density of both I_{so} and I_{to} varied markedly between individual atrial myocytes, even between cells from the same preparation. The frequency distribution, however, revealed a continuum in the I_{peak}/I_{late} relationship, suggesting that discrete cell groups do not exist for the relationship between I_{to} and I_{so}. Considering I_{to} and the delayed rectifier, Wang *et al.* (1993*a*) have formed three distinct groups depending on the relative magnitude between these two current components. When our data are analysed in such arbitrarily divided groups, we find similar group sizes. These results show that variations in outward current between cells of the human atria are a biological phenomenon. In human ventricle, I_{to} is larger in subepicardial than in subendocardial myocytes (Wettwer *et al.* 1994). It is therefore conceivable that the extremes of our relationships between I_{to} and I_{so} in atrial myocytes could be found also at either side of the atrial wall. However, direct evidence for such differences in outward currents within the human atrial wall requires further investigations using cells isolated from specific regions.

Comparison with cloned channels

Several genes encoding K^+ channel α-subunits have been recently cloned from human myocardium (Grupe *et al.* 1990; Tamkun *et al.* 1991; Fedida *et al.* 1993; Hice, Folander, Salata, Smith, Sanguinetti & Swanson, 1994). The diversity of clonal channel properties depends on the gene expressed, the expression system and possible heteromeric channel assembly (Po, Roberds, Snyders, Tamkun & Bennett, 1993). A comparison of the properties of currents following expression of these α-subunit genes and currents of human atrial and ventricular myocytes is summarized in Table 2.

Similarities between I_{so} and recently cloned human Kv1.5 channels. High correlation in kinetic and pharmacological properties between I_{so} and the currents following expression of two Kv1.5 channels, HK2 (Snyders, Tamkun & Bennett, 1993) and fHK (Fedida *et al.* 1993), suggest that these channels are putative clonal equivalents. Similarities were seen in both activation and inactivation kinetics, high sensitivity to 4-AP and relative insensitivity to TEA and DTX (Table 2). The resemblance in the kinetics of clofilium block of I_{so} (Amos, Li, Wettwer, Himmel, Metzger & Ravens, 1995) and Kv1.5 channels (Snyders *et al.* 1993; Malayev, Nelson & Philipson, 1995) provides further evidence. Due to the sensitivity of Kv1.6 channels to TEA, DTX and CTX (Grupe *et al.* 1990) and of I_{sK} to La^{3+} (Hice *et al.* 1994), these channels are not I_{so} equivalents.

The absence of I_{so} in human ventricular myocytes correlates with Northern blot analysis of HK2 mRNA expression (Tamkun *et al.* 1991), but not for fHK expression (Fedida *et al.* 1993). The level of mRNA encoding HK2 was

Table 2. Comparison of properties of native currents of human atrial and subepicardial ventricular myocytes with clonal channels and heterotetramers of clonal channels

Parameter	Activation $V_{0.5}$ (mV)	Inactivation τ (ms)	Inactivation $V_{0.5}$ (mV)	Recovery τ (ms)	4-AP IC_{50} (μM)	TEA IC_{50} (mM)	DTX IC_{50} (nM)	CTX IC_{50} (nM)	La^{3+}	Ba^{2+}
I_{to} atrium	+11·8 ± 1·0	61 ± 1	−36·7 ± 1·3	56 ± 8	1000	—	—	—	—	—
I_{to} ventricle	+10·5 ± 1·3	79 ± 2	−30·5 ± 1·1	24 ± 2	2690	—	?	?	?	?
I_{so}	+3·5 ± 2·2	1425 ± 26	−8·9 ± 0·9	?	6	—	—	—	—	—
Kv1.4[a]	−34·0 ± 0·7	35	−66·3 ± 3·1	3200 ± 400	700	—	?	?	?	?
Kv1.5[b]	−14·4 ± 4·0	~250 and ~2500	−25 ± 4	1650 ± 111	100	—	—	?	—	?
Kv1.6[c]	−20·8 ± 7·5	?	?	?	1500	7	20	1	?	?
I_{sK}[d]	+1·0 ± 1·9	—	—	—	?	?	?	?	+	?
Kv1.4/1.5[e] Hetero	?	~100	−26·2 ± 4·2	710 ± 100	2500	—	?	?	?	?
Kv1.4/1.2[e] Hetero	?	50	−41·4 ± 2·1	710 ± 100	790	—	?	?	?	?

Recovery, recovery from inactivation; 4-AP, 4-aminopyridine; TEA, tetraethylammonium; DTX, dendrotoxin; CTX, charybdotoxin; Hetero, heteromeric channel; ?, unknown; —, not observed or no significant effect; +, significant effect. Data for clonal channels from: a, Po, Snyders, Baker, Tamkun & Bennett (1992); b, Snyders *et al.* (1993); c, Grupe *et al.* (1990); d, Hice *et al.* (1994); e, Po *et al.* (1993).

10-fold greater in human atria than in human ventricle, whereas the level of fHK mRNA was easily detectable in both tissues. Undetectable I_{so} in human ventricle suggests absence or very low channel expression which is in accordance with low mRNA expression levels for HK2.

Heteromultimeric channel assembly for I_{to}? Under identical conditions, slight but significant differences in I_{to} inactivation kinetics and sensitivity to 4-AP block were observed between atrial and ventricular cells. One possible explanation for these observations may be different heteromeric channels underlying the two currents. It has been shown that co-expression of Kv1.4 α-subunits (I_{to} like) with Kv1.2 (I_{so} like) or Kv1.5 subunits (I_{so} like) in *Xenopus* oocytes results in I_{to}-like currents with slight but distinct differences in inactivation kinetics and sensitivities to 4-AP (Table 2; Po *et al.* 1993). The differences in inactivation kinetics between atrial and ventricular myocytes could also reflect different β-subunits between the tissues. β-Subunits have recently been cloned from human heart accelerating the inactivation of Kv1.4 and Kv1.5 currents (England, Uebele, Shear, Kodali, Bennett & Tamkun, 1995; Majumder, De Biasi, Wang & Wible, 1995). This would, however, seem less likely than different heteromeric channels, given the different 4-AP sensitivities. It should, however, be noted that marked discrepancy between native currents and the currents of clonal channels is found in the rate of recovery from inactivation (Table 2).

Conclusions

In atrial myocytes, outward current at 22 °C was the sum of a rapidly activating, slowly inactivating current (I_{so}), a rapidly activating, rapidly inactivating outward current (I_{to}) and a non-characterized, time-independent background current. I_{so} and I_{to} could be distinguished by different inactivation kinetics and sensitivity to 4-AP. In ventricular myocytes, only I_{to} and the background current could be detected. Thus the presence of I_{so} in atrial but not ventricular myocytes is a major factor in the generation of the shorter action potential duration of atrial myocardium. Slight but significant differences in the properties of I_{to} from atrial and ventricular myocytes were detected, suggesting that the channels responsible were not identical.

Agus, Z. S., Dukes, I. D. & Morad, M. (1991). Divalent cations modulate the transient outward current in rat ventricular myocytes. *American Journal of Physiology* **261**, C310–318.

Amos, G. J., Li, Q., Wettwer, E., Himmel, H. M., Metzger, F. & Ravens, U. (1995). Kinetics of clofilium block of human atrial outward currents. *Naunyn–Schmiedeberg's Archives of Pharmacology* **349**, R45 (abstract).

Apkon, M. & Nerbonne, J. M. (1991). Characterization of two distinct depolarization-activated K^+ currents in isolated adult rat ventricular myocytes. *Journal of General Physiology* **97**, 973–1011.

Backx, P. H. & Marban, E. (1993). Background potassium currents active during the plateau of the action potential in guinea pig ventricular myocytes. *Circulation Research* **72**, 890–900.

Beuckelmann, D. J., Näbauer, M. & Erdmann, E. (1993). Alterations of K^+ currents in isolated human ventricular myocytes from patients with terminal heart failure. *Circulation Research* **73**, 379–385.

Boyle, W. A. & Nerbonne, J. M. (1992). Two functionally distinct 4-aminopyridine-sensitive outward K^+ currents in rat atrial myocytes. *Journal of General Physiology* **100**, 1041–1067.

Canale, E. D., Campbell, G. R., Smolich, J. J. & Campbell, J. H. (1986). Cardiac muscle. In *The Handbook of Microscopic Anatomy*, ed. Oksche, A. & Vollrath, L., pp. 150–164. Springer-Verlag, Berlin, Heidelberg, New York, Tokyo.

CASTLE, N. A. & SLAWSKY, M. T. (1993). Characterization of 4-aminopyridine block of the transient outward current in adult rat ventricular myocytes. *Journal of Pharmacology and Experimental Therapeutics* **264**, 1450–1459.

DUKES, I. D. & MORAD, M. (1991). The transient K^+ current in rat ventricular myocytes: evaluation of its Ca^{2+} and Na^+ dependence. *Journal of Physiology* **435**, 395–420.

ENGLAND, S. K., UEBELE, V. N., SHEAR, H., KODALI, J., BENNETT, P. B. & TAMKUN, M. M. (1995). Characterization of a voltage-gated K^+ channel β subunit expressed in human heart. *Proceedings of the National Academy of Sciences of the USA* **92**, 6309–6313.

ESCANDE, D., COULOMBE, A., FAIVRE, J.-F., DEROUBAIX, E. & CORABOEUF, E. (1987). Two types of transient outward currents in adult human atrial cells. *American Journal of Physiology* **252**, H142–148.

FEDIDA, D., WIBLE, B., WANG, Z., FERMINI, B., FAUST, F., NATTEL, S. & BROWN, A. M. (1993). Identity of a novel delayed rectifier current from human heart with a cloned K^+ channel current. *Circulation Research* **73**, 210–216.

FOLLMER, C. H., LODGE, N. J., CULLINAN, C. A. & COLATSKY, T. J. (1992). Modulation of the delayed rectifier, I_K, by cadmium in cat ventricular myocytes. *American Journal of Physiology* **262**, C75–83.

FURUKAWA, T., KOUMI, S.-I., SAKAKIBARA, Y., SINGER, D. H., JIA, H., ARENTZEN, C. E. & WASSERSTROM, J. A. (1995). An analysis of lidocaine block of sodium current in isolated human atrial and ventricular myocytes. *Journal of Molecular and Cellular Cardiology* **27**, 831–846.

GOTOH, Y., IMAIZUMI, Y., WATANABE, M., SHIBATA, E. F., CLARK, R. B. & GILES, W. R. (1991). Inhibition of transient outward K^+ current by DHP Ca^{2+} antagonists and agonists in rabbit cardiac myocytes. *American Journal of Physiology* **260**, H1737–1742.

GRAJEK, S., LESIAK, M., PYDA, M., ZAJAC, M., PARADOWSKI, S. T. & KACZMAREK, E. (1993). Hypertrophy or hyperplasmia in cardiac muscle. Post-mortem human morphometric study. *European Heart Journal* **14**, 40–47.

GRUPE, A., SCHRÖTER, K. H., RUPPERSBERG, J. P., STOCKER, M., DREWES, T., BECKH, S. & PONGS, O. (1990). Cloning and expression of a human voltage-gated potassium channel. A novel member of the RCK potassium channel family. *EMBO Journal* **9**, 1749–1756.

HICE, R. E., FOLANDER, K., SALATA, J. J., SMITH, J. S., SANGUINETTI, M. C. & SWANSON, R. (1994). Species variants of the I_{sK} protein: differences in kinetics, voltage dependence, and La^{3+} block of the currents expressed in *Xenopus* oocytes. *Pflügers Archiv* **426**, 139–145.

HUME, J. R. & UEHARA, A. (1985). Ionic basis of the different action potential configurations of single guinea-pig atrial and ventricular myocytes. *Journal of Physiology* **368**, 525–544.

JIA, H., FURUKAWA, T., SINGER, D. H., SAKAKIBARA, Y., EAGER, S., BACKER, C., ARENTZEN, C. & WASSERSTROM, J. A. (1993). Characteristics of lidocaine block of sodium channels in single human atrial cells. *Journal of Pharmacology and Experimental Therapeutics* **264**, 1275–1284.

LIU, D. W., GINTANT, G. A. & ANTZELEVITCH, C. (1993). Ionic bases for electrophysiological distinctions among epicardial, mid-myocardial, and endocardial myocytes from the free wall of the canine left ventricle. *Circulation Research* **72**, 671–687.

MCCULLOUGH, J. R., CHUA, W. T., RASMUSSEN, H. H., TEN EICK, R. E. & SINGER, D. H. (1990). Two stable levels of diastolic potential at physiological K^+ concentrations in human ventricular myocardial cells. *Circulation Research* **66**, 191–201.

MAJUMDER, K., DE BIASI, M., WANG, Z. & WIBLE, B. A. (1995). Molecular cloning and functional expression of a novel potassium channel β-subunit from human atrium. *FEBS Letters* **361**, 13–16.

MALAYEV, A. A., NELSON, D. J. & PHILIPSON, L. H. (1995). Mechanism of clofilium block of human Kv1.5 delayed rectifier potassium channel. *Molecular Pharmacology* **47**, 198–205.

MEWES, T. & RAVENS, U. (1994). L-type calcium currents of human myocytes from ventricle of non-failing and failing hearts and from atrium. *Journal of Molecular and Cellular Cardiology* **26**, 1307–1320.

NÄBAUER, M., BEUCKELMANN, D. J. & ERDMANN, E. (1993). Characteristics of transient outward current in human ventricular myocytes from patients with terminal heart failure. *Circulation Research* **73**, 386–394.

PO, S., ROBERDS, S., SNYDERS, D. J., TAMKUN, M. M. & BENNETT, P. B. (1993). Heteromultimeric assembly of human potassium channels. Molecular basis of a transient outward current? *Circulation Research* **72**, 1326–1336.

PO, S., SNYDERS, D. J., BAKER, R., TAMKUN, M. M. & BENNETT, P. B. (1992). Functional expression of an inactivating potassium channel cloned from human heart. *Circulation Research* **71**, 732–736.

SAKAKIBARA, Y., FURUKAWA, T., SINGER, D. W., JIA, H., BACKER, C. L., ARENTZEN, C. E. & WASSERSTROM, J. A. (1993). Sodium current in isolated human ventricular myocytes. *American Journal of Physiology* **265**, H1301–1309.

SANGUINETTI, M. C., JIANG, C., CURRAN, M. E. & KEATING, M. T. (1995). A mechanistic link between an inherited and an acquired cardiac arrhythmia: *HERG* encodes the I_{Kr} potassium channel. *Cell* **81**, 299–307.

SANGUINETTI, M. C. & JURKIEWICZ, N. K. (1990). Two components of cardiac delayed rectifier K^+ current. Differential sensitivity to block by class III antiarrhythmic agents. *Journal of General Physiology* **96**, 195–215.

SANGUINETTI, M. C. & KASS, R. (1984). Voltage-dependent block of calcium channel current in the calf cardiac Purkinje fibre by dihydropyridine calcium antagonists. *Circulation Research* **55**, 336–348.

SCHNEIDER, M. W. & CHANDLER, W. K. (1976). Effects of membrane potential on the capacitance of skeletal muscle. *Journal of General Physiology* **67**, 125–163.

SHIBATA, E. F., DRURY, T., REFSUM, H., ALDRETE, V. & GILES, W. (1989). Contributions of a transient outward current to repolarization in human atrium. *American Journal of Physiology* **257**, H1773–1781.

SNYDERS, D. J., TAMKUN, M. M. & BENNETT, P. B. (1993). A rapidly activating and slowly inactivating potassium channel cloned from human heart. Functional analysis after stable mammalian cell culture expression. *Journal of General Physiology* **101**, 513–543.

STRONG, P. N. (1990). Potassium channel toxins. *Pharmacology and Therapeutics* **46**, 137–162.

TAMKUN, M. M., KNOTH, K. M., WALBRIDGE, J. A., KROEMER, H., RODEN, D. M. & GLOVER, D. M. (1991). Molecular cloning and characterization of two voltage-gated K^+ channel cDNAs from human ventricle. *FASEB Journal* **5**, 331–337.

TEN EICK, R. E. & SINGER, D. H. (1979). Electrophysiological properties of diseased human atrium. I. Low diastolic potential and altered cellular response to potassium. *Circulation Research* **44**, 545–557.

THURINGER, D., LAURIBE, P. & ESCANDE, D. (1992). A hyperpolarization-activated inward current in human myocardial cells. *Journal of Molecular and Cellular Cardiology* **24**, 451–455.

TRAUTWEIN, W., KASSEBAUM, D. G., NELSON, R. M. & HECHT, H. (1962). Electrophysiological study of human heart muscle. *Circulation Research* **10**, 306–312.

WANG, Z., FERMINI, B. & NATTEL, S. (1993*a*). Delayed rectifier outward current and repolarization in human atrial myocytes. *Circulation Research* **73**, 276–285.

WANG, Z., FERMINI, B. & NATTEL, S. (1993*b*). Sustained depolarization-induced outward current in human atrial myocytes. Evidence for a novel delayed rectifier K^+ current similar to Kv1.5 cloned channel currents. *Circulation Research* **73**, 1061–1076.

WETTWER, E., AMOS, G., GATH, J., ZERKOWSKI, R., REIDEMEISTER, J.-CH. & RAVENS, U. (1993). Transient outward current in human and rat ventricular myocytes. *Cardiovascular Research* **27**, 1662–1669.

WETTWER, E., AMOS, G. J., POSIVAL, H. & RAVENS, U. (1994). Transient outward current in human ventricular myocytes of subepi- and subendocardial origin. *Circulation Research* **75**, 473–482.

Acknowledgements

The authors wish to acknowledge the skilful technical assistance provided by Ms Sylvia Grunz, Barbara Langer, Iris Manthey and Doris Petermeyer. We also thank Professor Jürgen-Christoph Reidemeister, Professor Volker Sadony and Professor Reinhard Zerkowski of the Abteilung für Thorax- und kardiovaskuläre Chirurgie, Medizinische Einrichtungen der Universität-GH Essen, Essen, Germany, and Dr Herbert Posival from the Herzzentrum NRW der Ruhr-Universität Bochum, Bad Oeynhausen, Germany, for supplying the myocardial specimens.

Received 30 May 1995; accepted 29 August 1995.